

NEANDC (OR) - 140 "L"

INDC (SWT) - 6 "L"

PROGRESS REPORT TO NEANDC  
FROM SWITZERLAND

June 1974

T. Hürlimann

Swiss Federal Institute for Reactor Research  
Würenlingen

~~NOT FOR PUBLICATION~~

## PREFACE

This document contains information of a preliminary or private nature and should be used with discretion. Its contents may not be quoted, abstracted, or transmitted to libraries without the explicit permission of the originator.

## CONTENTS

	page
I. Institut de Physique, Université de Neuchâtel	3
II. Institut de Physique, Université de Fribourg	7
III. Eidgenössisches Institut für Reaktorforschung, Würenlingen	15
IV. Physikalisches Institut der Universität Zürich	22
V. Physikalisches Institut der Universität Basel	23
VI. Laboratorium für Kernphysik, Eidg. Technische Hochschule, Zürich	32
VII. Institut de Physique Nucléaire, Université de Lausanne	43

I. Institut de Physique, Université de Neuchâtel

(Dir.: Prof. Jean Rossel)

1. Phase shift and Mixing Parameters for the  
 $D(\vec{n},n)D$  Scattering at Low Energy

D. Bovet, S. Jaccard, R. Viennet and J. Weber

It has been found that fits of equal quality may be obtained by a splitting of the quartet phase shifts or by J-degenerate phase shifts and mixing parameters {1}.

Computations are in progress to obtain prediction of angular repartition of the Wolfenstein's parameters  $R$ ,  $R'$ ,  $A$  and  $A'$ . It is hoped that one of these will be more sensitive than the others to the type of model used for the analysis.

References

{1} Proceedings of the International Conference on Nuclear Physics, München 1973, Vol. 1, p. 331

D. Bovet, S. Jaccard and J. Weber

2. Neutron-Neutron Quasifree Scattering at 14.1 MeV\*

E. Bovet, F. Foroughi and J. Rossel

We have performed two breakup measurements from the  $D(n,2n)p$  reaction at 14.1 MeV in the region of n-n QFS ( $E_p \approx 0$ ). The neutron beam produced by the  $T(d,n)^4\text{He}$  reaction, using the associated  $\alpha$ -particle method {1}, is incident on a spherical  $\text{C}_6\text{D}_6$  target. The breakup neutrons are detected in two NE 213 liquid scintillators ( $15 \times 15 \times 4 \text{ cm}^3$ ) placed at 120 cm from

the target and at symmetric angles,  $\theta_{N1} = \theta_{N2}$ ,  $\phi_{12} = 180^\circ$ , around the beam axis. Since in our kinematical situation the energy of the proton passes through zero, it was not possible to detect the breakup proton in the target (used as a scintillator). Therefore particular attention was paid to other means of background reduction. In particular, n- $\gamma$  discrimination [2] was applied to the outputs of both neutron detectors and events due to moderated background neutrons were suppressed by electronic biases. Moreover we have taken advantage of the fact that at angles  $30^\circ \leq \theta_{N1,N2} \leq 50^\circ$ , a  $^{12}\text{C}$ -based deuterated compound used as a target does not produce any detectable contamination in the kinematical region of interest. Separate measurements with a graphite target have confirmed the absence of unwanted correlations from competing reactions. Moreover they have shown that the background outside the region of interest is the same as with the deuterated target (see fig. 1a).

The preliminary results are as follows (see fig. 1b):

- 1) the differential cross section at  $\theta_{N1} = \theta_{N2} = 30^\circ$  is compatible with that obtained by Slaus et al. [3], within the limits of experimental uncertainties which are still rather large in both experiments;
  - 2) the differential cross section at  $\theta_{N1} = \theta_{N2} = 40^\circ$  (exact pole location  $E_p = 0$ ) is approximatively 3 times smaller than that at  $30^\circ$  ( $E_p = 180$  keV). This drop is similar to though more marked than that found in the  $D(p,2p)n$  reaction [4].
- More definitive measurements are in progress with a  $\text{C}_6\text{D}_{12}$  target.

#### References

- [1] C. Lunke, J. P. Egger and J. Rossel, Nucl. Phys. A158, 278 (1970)
- [2] E. Bovet, P. Boschung and J. Rossel, Nucl. Instr. and Meth. 101, 315 (1972)

- {3} I. Slaus, J. W. Sunier, G. Thompson, J. C. Young,  
J. W. Verba, D. J. Margaziotis, P. Doherty and R. T. Cahill,  
Phys. Rev. Lett. 26, 789 (1971)
- {4} E. Andrad, V. Valkovic, D. Rendic and G. C. Phillips,  
Nucl. Phys. A183, 145 (1972)

\* A more detailed paper has been submitted for publication  
in Phys. Rev. Lett.

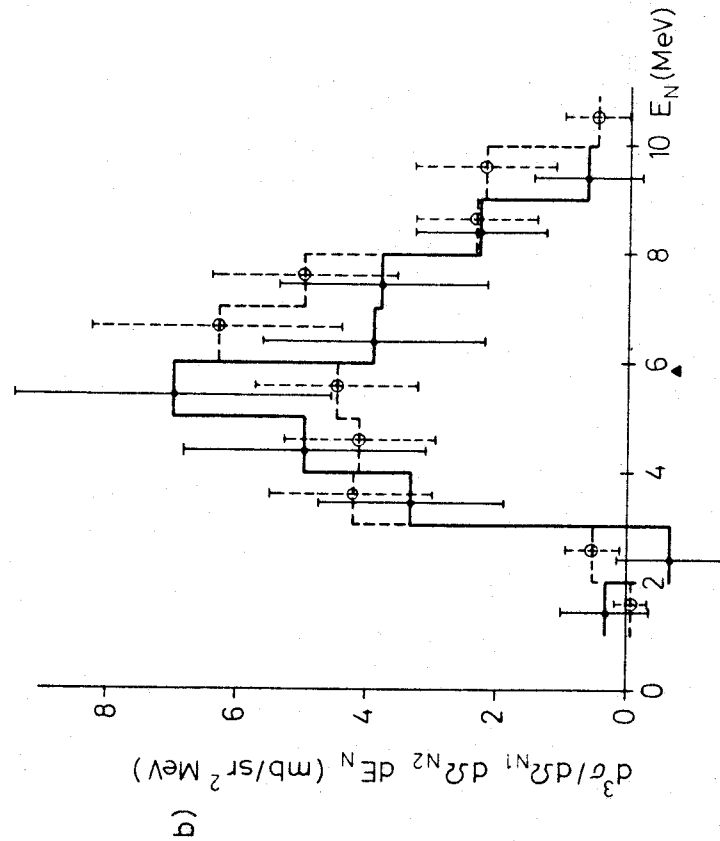
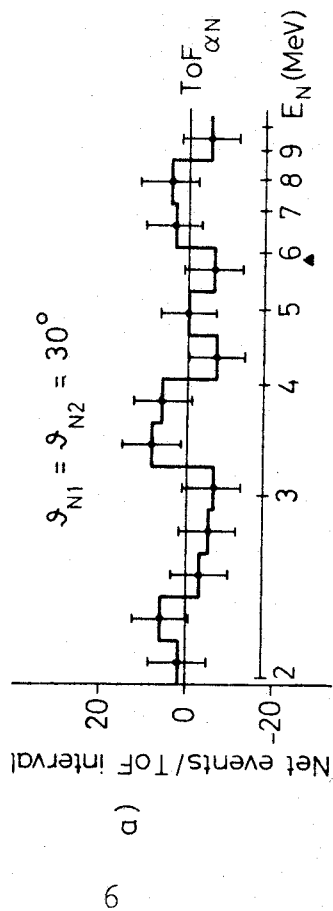


Fig. 1a :

Projections on the  $\text{ToF}_{\alpha-N}$  axis of the difference between the background obtained both with the  $\text{C}_6\text{D}_6$  target (interpolated under the QFS kinematical region) and with the graphite target. The difference is seen to be zero to within experimental uncertainty. The triangles indicate the points corresponding to  $E_p \approx 180 \text{ keV}$  ( $30^\circ$ ), resp.  $E_p \approx 0$  ( $40^\circ$ ).

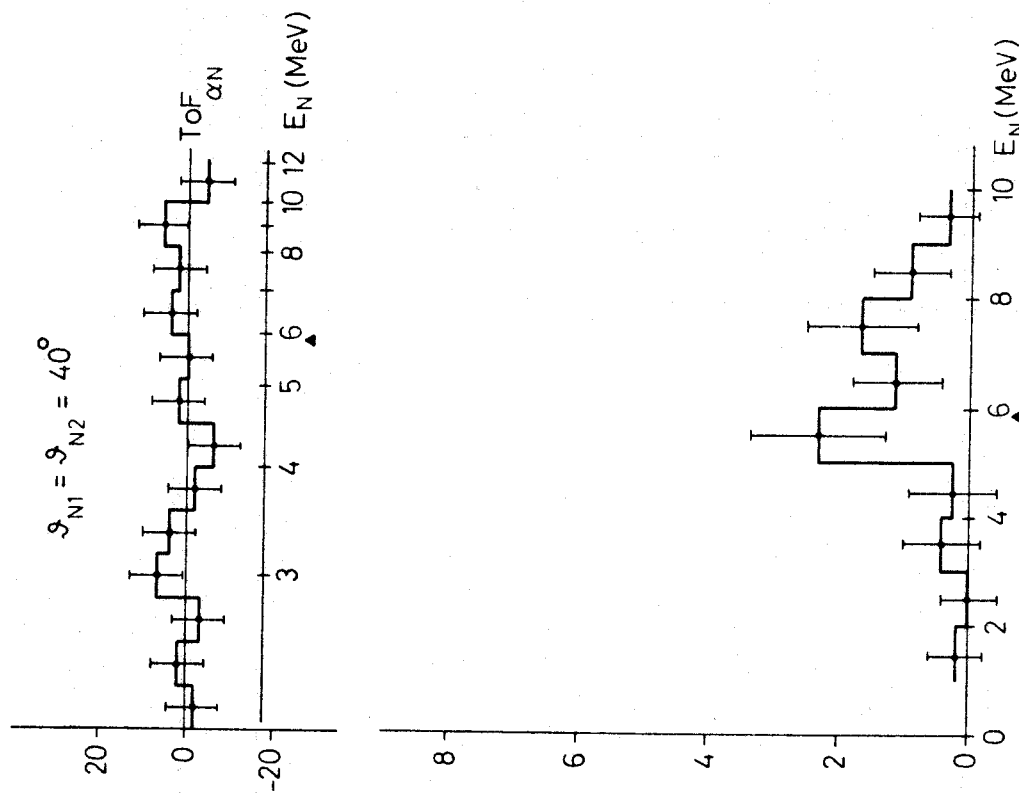


Fig. 1b :

Projections of the breakup events on the neutron energy axis. The solid line histograms represent our measurements. Besides statistical uncertainties, the error bars comprise uncertainties in the angular resolution and the detector efficiency. The broken line histogram is that of Slaus et al. {3}.

(Dir.: Prof. Dr. O. Huber)

1. Study of the levels in  $^{233}\text{Th}$  using the  $^{232}\text{Th}(n,\gamma)$  reaction\*

Jean Kern and D. Duc

A total of 112 gamma rays of the reaction  $^{232}\text{Th}(n,\gamma)^{233}\text{Th}$  have been observed with the Fribourg pair spectrometer in the energy range  $2.48 < E_\gamma < 4.8$  MeV. This apparatus has been described previously [1].

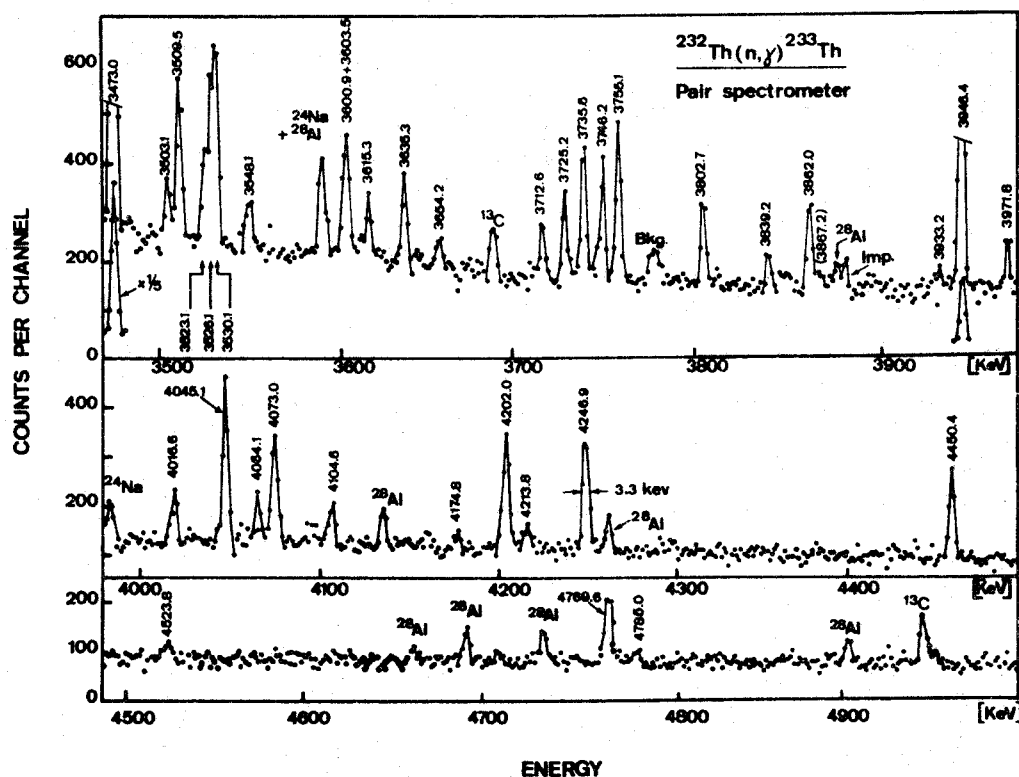


Fig. 1: Portion of the high energy  $^{232}\text{Th}(n,\gamma)$  spectrum taken in pair mode with the 20 cm<sup>3</sup> Ge(Li) detector. The solid line serves only as a guide to the eye. Identified impurities are noted. The label "Bkg" is given to an unidentified peak observed in a background run, the label "Imp" to a peak not present in the other measurements.

Two sets of experiments have been performed, one with a planar  $3 \text{ cm}^3 \text{ Ge(Li)}$  detector, the second, with a coaxial  $20 \text{ cm}^3 \text{ Ge(Li)}$  diode. As shown in fig. 1, the energy resolution was  $3.3 \text{ keV}$  FWHM for  $4.2 \text{ MeV}$  transitions in the second set.

The experiments were performed at the throughtube facility of the reactor SAPHIR in Würenlingen (EIR). At the external target position, the thermal neutron flux was about  $3 \times 10^7 \text{ n / cm}^2 \text{ s}$ .

The level scheme proposed in previous works {2}{3} has been extended. A value of  $4786.35 \pm 0.25 \text{ keV}$  has been determined for the neutron binding energy in  $^{233}\text{Th}$ .

#### References

- {1} B. Michaud, J. Kern, L. Ribordy and L. A. Schaller, *Helv. Phys. Acta* 45 (1972) 93
- {2} T. Grottdal, J. Limstrand, K. Nybø, K. Skår<sup>0</sup> and T. F. Thorsteinsen, *Nucl. Phys.* A189 (1972) 592
- {3} T. von Egidy, O. W. B. Schult, D. Rabenstein, J. R. Erskine, O. A. Wasson, R. E. Chrien, D. Breitig, R. P. Sharma, H. A. Baader, H. R. Koch, *Phys. Rev.* C6 (1972) 266

\* Work supported by the Fonds National Suisse de la Recherche Scientifique



## 2. Neutron Capture $\gamma$ -rays in $^{238}\text{Np}^*$

V. A. Ionescu and J. Kern

The neutron capture gamma rays following the reaction  $^{237}\text{Np}(n,\gamma)^{238}\text{Np}$  have been investigated. The measurements were performed in an external target geometry at the tangential beam channel of the reactor SAPHIR of the Swiss Federal Institute for Reactor Research ( $\Phi \approx 2 \times 10^7 \text{ n/cm}^2 \text{ s}$  at target position).

The high energy spectrum has been investigated in the range 2600-5500 keV. The measurements were performed with a Ge(Li)-NaI(Tl) pair spectrometer [1]. The existence of 71 transitions has been established with an energy accuracy ranging between  $0.15 \div 0.18 \text{ keV}$ . Figure 1 presents a portion of high energy spectrum.

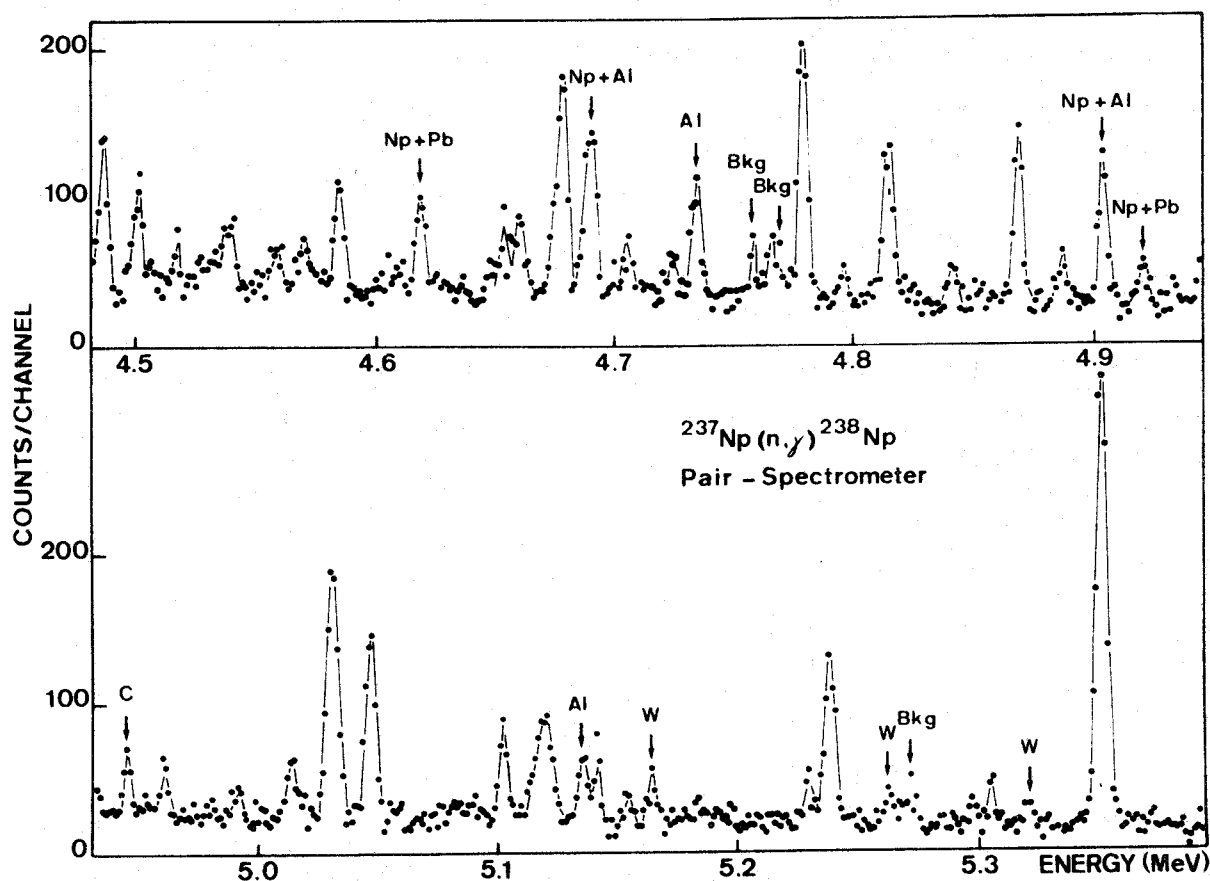


Fig. 1: High energy portion of the  $^{237}\text{Np}(n,\gamma)^{238}\text{Np}$  spectrum

The low energy spectra have been measured with the same detectors operated as an anticompton spectrometer up to 1500 keV and with a 2.4 cm<sup>3</sup> high resolution Ge(Li) detector {2} in the range 0 ÷ 700 keV. Special care was taken to separate the low energy neutron capture gamma rays from the accompanying radioactivity of <sup>237</sup>Np, <sup>238</sup>Np and <sup>233</sup>Pa. The existence of about 60 low energy transitions was established with an accuracy ranging between .030 ÷ 0.15 keV.

The neutron separation energy has been determined.

#### References

- {1} B. Michaud, J. Kern, L. Ribordy, L. A. Schaller,  
Helv. Phys. Acta 45 (1972) 93
- {2} We thank Prof. H. J. Leisi (ETH Zürich) for lending us  
this detector

\* Work supported by the Fonds National Suisse de la  
Recherche Scientifique

3. Study of the  $^{241}\text{Am} (n, \gamma) ^{242}\text{Am}$  reaction using a pair spectrometer\*

M. Gasser and J. Kern

The  $\gamma$ -rays following the thermal neutron capture in  $^{241}\text{Am}$  have been measured with the Fribourg pair spectrometer [1], but using a coaxial 20 cm<sup>3</sup> Ge(Li) diode as the central detector. The use of this larger diode and of an improved electronic setup resulted both in a better detection efficiency and better energy resolution [2].

The target consisted of 1.1g  $\text{Am}_2\text{O}_3$  powder, i. e. 3.4 Ci  $^{241}\text{Am}$ . The measurements have been performed on the reactor SAPHIR in Würenlingen. The target was exposed to a thermal neutron flux of about  $2 \cdot 10^7$  n/cm<sup>2</sup> s for about 90 hours. A portion of the  $\gamma$ -spectrum is shown in fig. 1.

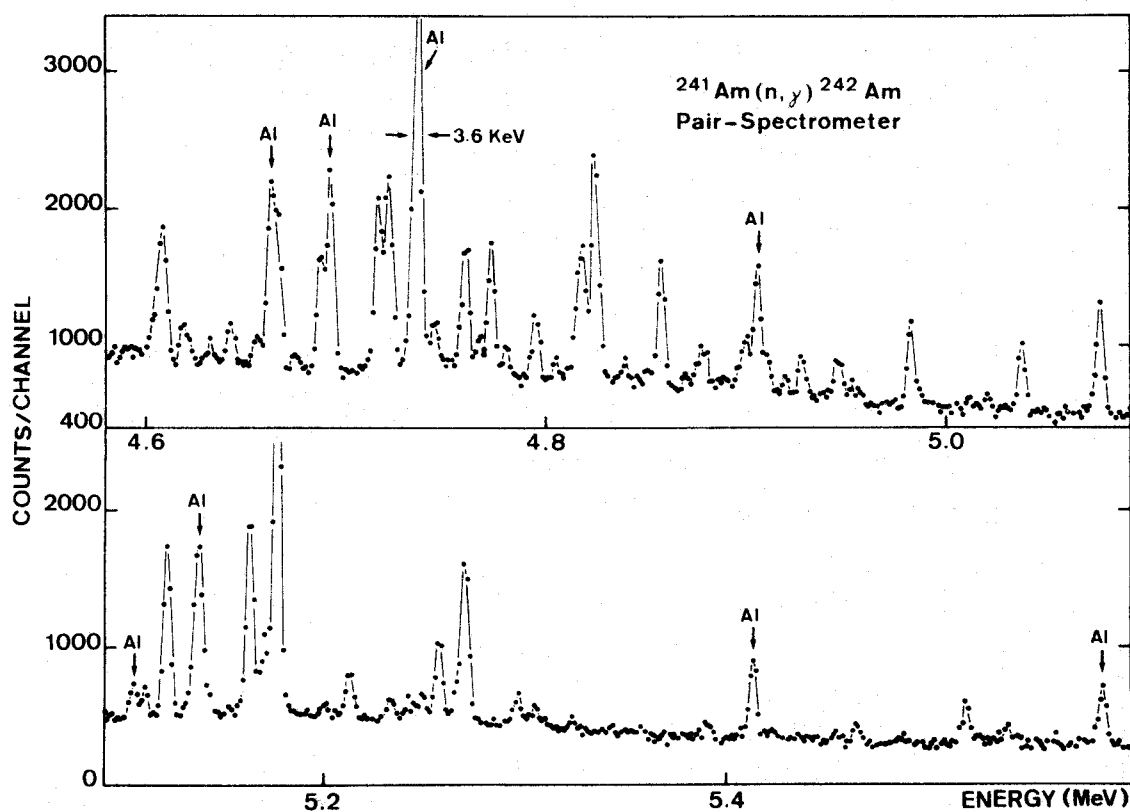


Fig. 1: Portion of the  $^{241}\text{Am} (n, \gamma) ^{242}\text{Am}$  spectrum taken with a pair spectrometer. The time of measurement was about 90 hours

Intense lines from the  $^{27}\text{Al}$  (n, $\gamma$ ) reaction originate from the thin walled aluminium box containing the  $\text{Am}_2\text{O}_3$  powder. These Al-lines were employed for energy calibration purposes. The complex spectrum has been analyzed in the region of 4.5 to 5.5 MeV (Q-value: 5.475 MeV). About 60  $\gamma$ -lines could be attributed to the  $^{241}\text{Am}$  (n, $\gamma$ )  $^{242}\text{Am}$  reaction. Energies and intensities of these lines have been determined. In order to establish a reliable level scheme data from experiments like (d,p), (n, $e^-$ ), low energy (n, $\gamma$ ) etc are needed.

#### References

- {1} B. Michaud, J. Kern, L. Ribordy and L. A. Schaller,  
Helv. Phys. Acta 45 (1972) 93
- {2} M. Gasser, O. Huber, V. Ionescu, J. Kern and A. Raemy,  
Helv. Phys. Acta 45 (1972) 925

\* Work supported by the Fonds National Suisse de la  
Recherche Scientifique

#### 4. Nuclear Levels in $^{160}\text{Tb}^*$

Jean Kern, G. Mauron, B. Michaud

The high energy  $\gamma$ -ray spectrum from thermal neutron capture in natural terbium has been observed over the range of 5200 to 6400 keV with the Fribourg pair spectrometer. This apparatus, whose main component is a  $3\text{ cm}^3\text{ Ge(Li)}$  diode surrounded by a 20 cm diameter  $\text{NaI(Tl)}$  scintillator has been described previously [1]. The resolution obtained in the two main experiments are 4.0 keV and 5.2 keV FWHM for the 6218 keV transition (see fig. 1).

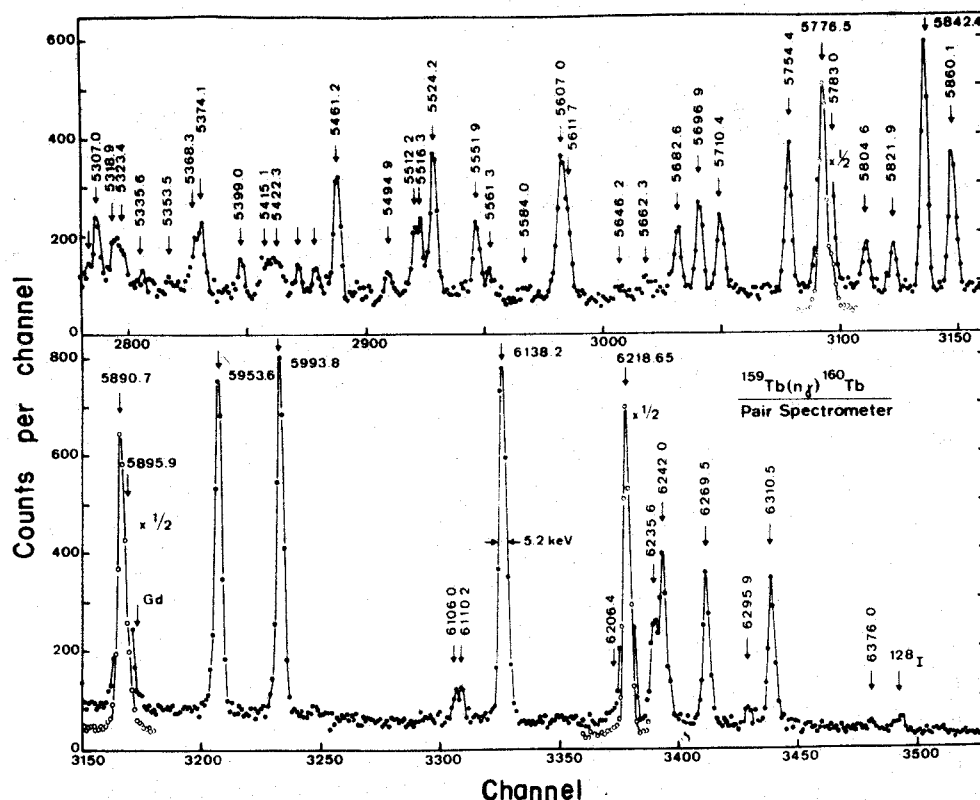


Fig. 1: A portion of the high energy  $^{159}\text{Tb}(n,\gamma)$  spectrum observed with the Fribourg pair spectrometer

The same reaction has been studied over the range 22 to 1230 keV with an anti-Compton spectrometer, which uses the same components as the pair spectrometer, but different logic circuitry. The reactor SAPHIR in Würenlingen was used as the neutron source in the two experiments.

The data have been combined with a previous  $^{159}\text{Tb}(d,p)$  investigation {2} and with the results obtained in the study of the  $(n,\gamma)$ ,  $(n,e^-)$  and  $(n,\gamma-\gamma)$  reactions in other laboratories. A level scheme has been constructed. Nine rotational bands built on two quasi-particle configurations have been disclosed.

A full account of the results has been published recently {3}.

#### References

- {1} B. Michaud, J. Kern, L. Ribordy and L. A. Schaller, *Helv. Phys. Acta* 45 (1972) 93
- {2} G. L. Struble and R. K. Sheline, *Sov. J. Nucl. Phys.* 5 (1967) 862
- {3} J. Kern, G. Mauron, B. Michaud, K. Schreckenbach, T. von Egidy, W. Mampe, H. R. Koch, H. A. Baader, D. Breitig, U. Gruber, B. P. K. Maier, O. W. B. Schult, J. T. Larsen and R. G. Lanier, *Nucl. Phys.* A221 (1974) 333

\* Work supported by the Fonds National Suisse de la Recherche Scientifique

1. Mass Distribution in Neutron Induced Fission

M. Rajagopalan, H. S. Pruys, A. Grütter,

H. R. von Gunten, E. A. Hermes, E. Roessler and

A. Schmid

A. Fission of  $^{235}\text{U}$  and  $^{239}\text{Pu}$  induced by fast neutrons from the reactor PROTEUS:

The yields of the fission products in the fission of  $^{235}\text{U}$  and  $^{239}\text{Pu}$  induced by fast neutrons in the core of the reactor PROTEUS are reported here. The yields were determined by a comparison method using gamma spectroscopy. The intensities of fission product gamma rays were determined in both the fast neutron and thermal neutron induced fission of  $^{235}\text{U}$  and from the known yields in the thermal neutron induced fission of  $^{235}\text{U}$ , the relative yields in the fast fission were calculated. The same procedure was adopted for  $^{239}\text{Pu}$  fission also. Two methods were adopted for gamma spectroscopy. In method A, the gamma ray intensities were measured directly after irradiation of the targets. In method B, the target material (U or Pu) was chemically separated before taking the gamma spectra of fission products so that the gamma rays from the target material did not interfere with the determination of fission product gamma ray intensities. The yields from both methods were normalized relative to the chain yield of mass number 140. The yields for  $^{235}\text{U}$  and  $^{239}\text{Pu}$  are given in Table I. For  $^{235}\text{U}$  the relative yields were converted to absolute yields by normalizing the total yield of all fission products to 200 %. The errors quoted include both statistical and systematic errors. For  $^{239}\text{Pu}$  the yields quoted are relative yields and were obtained by normalizing the yields with respect to  $^{140}\text{Ba}$ . The yield of  $^{140}\text{Ba}$  was

assumed to be 5.50 %. The errors quoted are only statistical errors. The yields quoted for  $^{239}\text{Pu}$  are only preliminary values. Further work on  $^{239}\text{Pu}$  is in progress.

B. Fission of  $^{238}\text{U}$  induced by 14 MeV neutrons:

Mass distribution in the fission of  $^{238}\text{U}$  induced by 14 MeV neutrons was determined using gamma spectroscopy. The relative fission yields in the 14 MeV neutron induced fission are given in Table II. For fission products designated with a \*, the yields were determined from the known efficiency of the detector and the known intensity ratios of gamma lines of specific fission products. For other fission products, the yields were determined by comparing the intensities with those in thermal neutron fission. All the yields were normalized to the yields of  $^{140}\text{Ba}$  which was assumed to be 4.56 %. These are only preliminary results obtained by taking gamma spectra after chemical separation of target material. For some fission products more accurate yields can be obtained by direct measurement of gamma ray intensities and such measurements are in progress.



Table I

Yields in fast neutron induced fission (PROTEUS-Reactor)

Mass No.	Element	$^{235}\text{U}$ Fission		$^{239}\text{Pu}$ Fission	
		Yield in %	Method	Yield in %	Method
87	Kr	$2.66 \pm 0.11$	B	---	
88	Kr,Rb	$4.45 \pm 0.26$	B	---	
91	Sr,Y	$5.63 \pm 0.21$	A+B	$2.57 \pm 0.09$	A+B
92	Sr,Y	$5.77 \pm 0.21$	A+B	$3.01 \pm 0.08$	A+B
93	Y	$6.23 \pm 0.21$	A+B	$3.49 \pm 0.13$	A
94	Y	$6.13 \pm 0.26$	A	---	
95	Zr	$6.49 \pm 0.25$	B	$5.96 \pm 0.24$	B
97	Zr,Nb	$5.97 \pm 0.19$	B	$5.67 \pm 0.47$	B
99	Mo,Tc	$6.23 \pm 0.22$	A	$6.08 \pm 0.20$	A+B
101	Tc	$5.31 \pm 0.18$	A	$7.20 \pm 0.60$	B
103	Ru	$3.20 \pm 0.12$	A	$6.85 \pm 0.23$	A+B
104	Tc	$1.87 \pm 0.08$	A	---	
105	Ru	$1.10 \pm 0.04$	A	$5.25 \pm 0.08$	A+B
129	Sb	$1.08 \pm 0.07$	C	---	
131	I	$3.06 \pm 0.10$	B	---	
132	I	$4.59 \pm 0.15$	B	$5.46 \pm 0.25$	B
133	I	$7.08 \pm 0.22$	B	$7.66 \pm 0.78$	B
134	I	$7.77 \pm 0.26$	B	$6.42 \pm 0.36$	B
135	I	$7.02 \pm 0.22$	B	$7.43 \pm 0.26$	B
139	Ba	$6.52 \pm 0.21$	A	$5.64 \pm 0.40$	B
140	Ba,La	$6.27 \pm 0.23$	A	5.50(Ref)	A+B
141	Ba,Ce	$5.52 \pm 0.34$	A	$5.81 \pm 0.04$	A
142	La	$5.74 \pm 0.32$	A+B	$5.16 \pm 0.19$	A+B
143	Ce	$5.70 \pm 0.21$	A+B	$4.46 \pm 0.31$	A+B
146	Pr	$2.75 \pm 0.14$	A	---	
147	Nd	$2.26 \pm 0.74$	A	$1.95 \pm 0.05$	A
149	Nd	$1.05 \pm 0.04$	A	$1.24 \pm 0.26$	A+B
151	Pm	$0.43 \pm 0.02$	A	$0.82 \pm 0.15$	A

A: Gamma counting after chemical separation of target material

B: Direct gamma counting after irradiation

C: Radiochemical separation

Table II

Yields in the 14 MeV neutron induced fission of  $^{238}\text{U}$ 

Mass No.	Element	Cumulative yield
91	Sr,Y	$3.63 \pm 0.08$
92	Sr,Y	$3.81 \pm 0.08$
93	Y	$4.36 \pm 0.08$
99	Mo	$5.42 \pm 0.08$
101	Tc	$4.81 \pm 0.10$
103	Ru	$4.57 \pm 0.14$
105	Ru	$3.14 \pm 0.12$
112	Ag	$0.56^{*\pm} 0.09$
113	Ag	$0.91^{*\pm} 0.14$
115	Cd	$0.79^{*\pm} 0.12$
117	Cd	$0.70^{*\pm} 0.11$
139	Ba	$5.00 \pm 0.18$
140	Ba	$4.56(\text{Ref})$
141	Ce	$4.03 \pm 0.08$
142	La	$3.85 \pm 0.08$
143	Ce	$3.69 \pm 0.10$
147	Nd	$1.98 \pm 0.26$
149	Nd	$1.34 \pm 0.08$
151	Pm	$0.78 \pm 0.02$
156	Sm	$0.14^{*\pm} 0.02$

\* Direct Determinations

## 2. The Decay of $^{152\text{m}1}\text{Eu}$ and $^{152\text{m}2}\text{Eu}$

H. S. Pruys, E. A. Hermes, H. R. von Gunten

Energies and intensities of the  $\gamma$ -rays in the decay of  $^{152\text{m}1}\text{Eu}$  and  $^{152\text{m}2}\text{Eu}$  have been determined.  $\gamma$ -spectra above 200 keV and below 200 keV were measured with a 40 cm<sup>3</sup> Ge(Li) detector and a 5 cm<sup>3</sup> planar pure Ge detector respectively. An example of a  $\gamma$ -ray spectrum obtained with the Ge detector is shown in fig. 1.

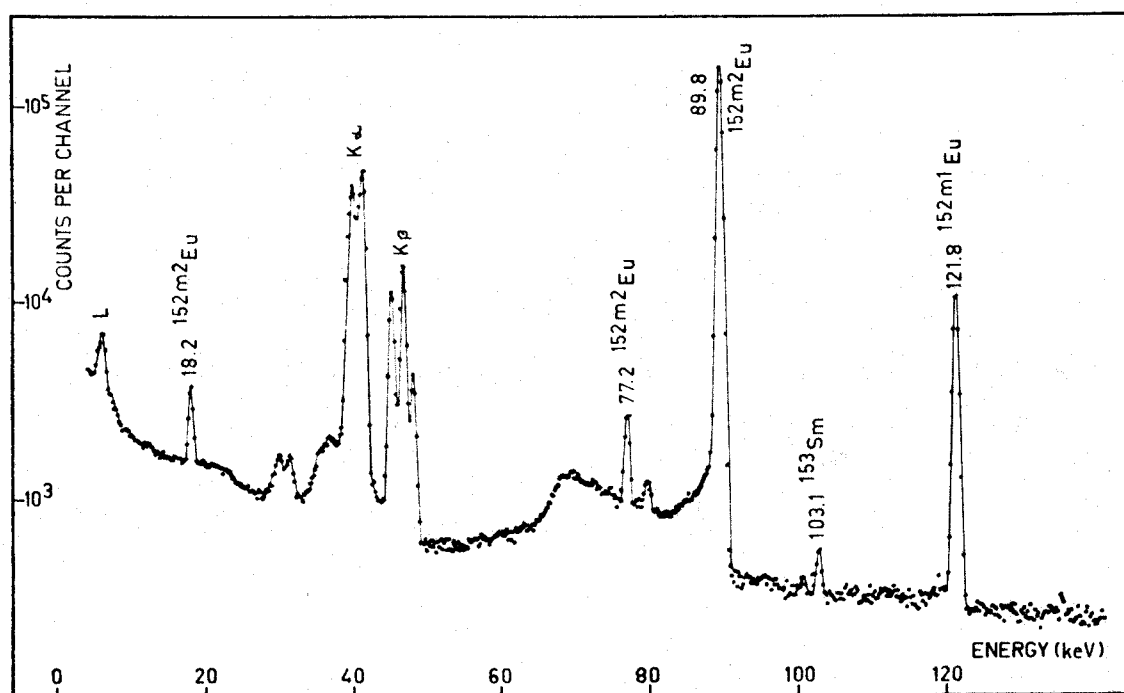


Fig. 1:  $\gamma$ -ray spectrum of 14 MeV neutron produced  $^{152\text{m}2}\text{Eu}$

Enriched  $^{151}\text{Eu}$ - and  $^{153}\text{Eu}$ -oxyde samples were irradiated with thermal neutrons and 14 MeV neutrons in order to obtain sources of  $^{152\text{m}1}\text{Eu}$  and  $^{152\text{m}2}\text{Eu}$ . The ratio of the activities of  $^{152\text{m}2}\text{Eu}/^{152\text{m}1}\text{Eu}$  was much higher in the 14 MeV neutron irradiation.

The  $\gamma$ -ray energies and intensities measured in the decay of  $^{152\text{m}1}\text{Eu}$  are presented in table 1. The results are in very good agreement with those of Barrette et al. [1]. In their work five

more  $\gamma$ -lines were detected, but only two of them could be placed in the decay scheme. The intensities reported by Ardisson et al. {2} are in considerable disagreement with the work of Barrette et al. {1} and the present work. Nine new  $\gamma$ -lines were observed by Ardisson et al. {2}, but according to our work six of them are sum peaks. The existence of the 1756.2 keV level in  $^{152}\text{Gd}$  {1} has been confirmed by our coincidence measurements since the 1411.88 keV  $\gamma$ -line was detected in coincidence with the 344.25 keV transition.

Table 1 : ENERGIES AND RELATIVE INTENSITIES OF THE  $\gamma$ -RAYS EMITTED IN THE DECAY OF  $^{152m1}\text{Eu}$

$E_{\gamma}$ (keV)			$I_{\gamma}$		
this work	Barrette et al. 1)	Ardisson et al. 2)	this work	Barrette et al. 1)	Ardisson et al. 2)
121.75 $\pm$ 0.04	121.78 $\pm$ 0.03		311 $\pm$ 10	295 $\pm$ 15	410 $\pm$ 41
244.65 $\pm$ 0.06	244.66 $\pm$ 0.03	244.7 $\pm$ 0.5	0.94 $\pm$ 0.06	1.00 $\pm$ 0.15	1.42 $\pm$ 0.18
271.16 $\pm$ 0.06	271.2 $\pm$ 0.2	270.0 $\pm$ 0.5	3.39 $\pm$ 0.12	3.40 $\pm$ 0.25	4.4 $\pm$ 0.5
344.25 $\pm$ 0.04	344.31 $\pm$ 0.3		100	100	143 $\pm$ 7
443.94 $\pm$ 0.06	443.98 $\pm$ 0.05	444.5 $\pm$ 1.0	0.99 $\pm$ 0.12	1.07 $\pm$ 0.12	1.53 $\pm$ 0.24
547.4 $\pm$ 0.3	547.5 $\pm$ 0.5		0.35 $\pm$ 0.06	0.4 $\pm$ 0.2	
563.00 $\pm$ 0.04	562.99 $\pm$ 0.07	563.0 $\pm$ 0.5	9.0 $\pm$ 0.3	9.2 $\pm$ 0.5	10.5 $\pm$ 1.2
586.3 $\pm$ 0.2	586.5 $\pm$ 0.2		0.47 $\pm$ 0.05	0.4 $\pm$ 0.2	
688.70 $\pm$ 0.06	688.68 $\pm$ 0.08	688.6 $\pm$ 0.5	2.63 $\pm$ 0.12	2.7 $\pm$ 0.4	2.3 $\pm$ 0.24
699.33 $\pm$ 0.06	699.28 $\pm$ 0.15	698.8 $\pm$ 0.5	2.98 $\pm$ 0.18	2.7 $\pm$ 0.5	3.4 $\pm$ 0.4
703.55 $\pm$ 0.06	703.6 $\pm$ 0.2	703.4 $\pm$ 0.5	2.51 $\pm$ 0.18	2.6 $\pm$ 0.4	3.1 $\pm$ 0.3
810.47 $\pm$ 0.08	810.7 $\pm$ 0.3	810.1 $\pm$ 0.8	1.05 $\pm$ 0.06	0.97 $\pm$ 0.20	1.18 $\pm$ 0.24
826.01 $\pm$ 0.07	826.0 $\pm$ 0.2	825.9 $\pm$ 0.6	1.23 $\pm$ 0.12	1.20 $\pm$ 0.15	1.12 $\pm$ 0.24
841.62 $\pm$ 0.05	841.68 $\pm$ 0.08	841.4 $\pm$ 0.3	585 $\pm$ 18	595 $\pm$ 20	590
870.14 $\pm$ 0.06	870.15 $\pm$ 0.12	869.8 $\pm$ 0.5	3.63 $\pm$ 0.18	3.9 $\pm$ 0.4	3.6 $\pm$ 0.4
963.39 $\pm$ 0.05	963.36 $\pm$ 0.08	963.4 $\pm$ 0.3	487 $\pm$ 16	492 $\pm$ 15	490 $\pm$ 30
970.36 $\pm$ 0.07	970.34 $\pm$ 0.10	970.1 $\pm$ 0.3	25.2 $\pm$ 1.3	25.3 $\pm$ 0.8	43 $\pm$ 5
995.85 $\pm$ 0.08	995.77 $\pm$ 0.12	995.6 $\pm$ 0.5	2.69 $\pm$ 0.12	2.7 $\pm$ 0.3	2.8 $\pm$ 0.3
1314.65 $\pm$ 0.07	1314.58 $\pm$ 0.06	1314.5 $\pm$ 0.4	40.4 $\pm$ 1.3	39.4 $\pm$ 1.2	48 $\pm$ 4
1389.11 $\pm$ 0.07	1389.02 $\pm$ 0.06	1388.9 $\pm$ 0.3	35.0 $\pm$ 1.1	33.0 $\pm$ 1.0	34 $\pm$ 4
1411.88 $\pm$ 0.10	1411.77 $\pm$ 0.10	1411.5 $\pm$ 0.4	1.87 $\pm$ 0.06	1.82 $\pm$ 0.12	2.4 $\pm$ 0.3
1510.80 $\pm$ 0.10	1510.75 $\pm$ 0.20	1510.6 $\pm$ 0.5	0.27 $\pm$ 0.03	0.35 $\pm$ 0.10	1.36 $\pm$ 0.18
1558.90 $\pm$ 0.15	1558.78 $\pm$ 0.20	1558.7 $\pm$ 1.0	0.35 $\pm$ 0.02	0.36 $\pm$ 0.07	0.31 $\pm$ 0.06
1680.8 $\pm$ 0.2	1680.6 $\pm$ 0.3	1681.0 $\pm$ 1.0	0.27 $\pm$ 0.02	0.22 $\pm$ 0.05	0.25 $\pm$ 0.06
1756.2 $\pm$ 0.2	1755.6 $\pm$ 0.5	1755.8 $\pm$ 1.5	0.12 $\pm$ 0.03	0.09 $\pm$ 0.03	0.20 $\pm$ 0.06

The results of the measurements of the  $^{152m2}\text{Eu}$  decay are presented in table 2. The  $\gamma$ -ray energies are in agreement with the values reported in the electron conversion work of Takahashi et al. {3}. The K-shell internal conversion coefficient for the 89.82 keV transition was deduced from the measured K X-ray intensity. The value for  $\alpha_K$ ,  $0.28 \pm 0.03$ , is in agreement with previously reported values of  $0.27 \pm 0.04$  {4} and  $0.30 \pm 0.05$  {3}. The 77.23 keV  $\gamma$ -line found in our work was assigned to  $^{152m2}\text{Eu}$  on basis of its half life.

The half-lives of  $^{152m1}\text{Eu}$  and  $^{152m2}\text{Eu}$  have been measured to be  $9.30 \pm 0.05$  h and  $96 \pm 1$  min respectively in agreement with the values given in the Chart of the Nuclides {5}.

Table 2:  $\gamma$ -rays from the decay of  $^{152m2}\text{Eu}$

$E_\gamma$ (keV)		relative intensity
this work	Takahashi et al. {3}	
$18.21 \pm 0.04$	$18.25 \pm 0.10$	$1.63 \pm 0.11$
$77.23 \pm 0.04$		$0.95 \pm 0.07$
$89.82 \pm 0.04$	$89.83 \pm 0.15$	100

#### References

- {1} J. Barrette, M. Barette, A. Boutard, G. Lamoureux, S. Monaro, S. Markiza, Can. J. Phys. 49 (1971) 2462
- {2} G. Ardisson, F. Armanet, A. Al Foudi, Compt. Rend. Ser B 274 (1972) 1436
- {3} K. Takahashi, M. McKeown, G. Scharff-Goldhaber, Phys. Rev. 137B (1965) 763
- {4} P. Kirkby, T. M. Kavanagh, Nucl. Phys. 49 (1963) 300
- {5} W. Seelmann-Eggebert, G. Pfennig, H. Münzel, Nuklidkarte, 3. Auflage, Bundesminister für wissenschaftliche Forschung, Bonn (1968)

IV. Physikalisches Institut der Universität Zürich

(Prof. Dr. Verena Meyer)

Current experiments on Van de Graaff Accelerators:

1. Precision measurements of p-p scattering phases at energies below 10 MeV

Measurements of the differential scattering cross-section in the energy range 320-450 keV are being made with an accuracy of approx. 1/2 %.

2. Nuclear spectroscopy with high energy resolution

With the aid of high resolution ( $\Delta E \leq 500$  eV) elastic scattering an investigation is being made of nuclear states with regard to the statistics of level densities and analogue resonances. Protons are scattered elastically by  $^{32}\text{S}$  ( $T=3/2$  state),  $^{50}\text{Cr}$  and  $^{54}\text{Fe}$  (analogue states and level densities) and  $^{92}\text{Mo}$  (analogue states at  $E_p = 4.36$  and  $5.3$  MeV). Energy range  $E_p = 3.0-5.4$  MeV.

3. Measurement of short lifetimes ( $< 1\text{ns}$ )

The lifetimes of states in  $^{13}\text{C}$ ,  $^{16}\text{O}$  and  $^{39}\text{K}$  were measured with the aid of a high resolution pulsed particle beam ( $\Delta t \leq 100\text{ps}$ ).

1. Analyzing Power of  $\vec{n}$ -p-Scattering at 14.2 MeV

B. Leemann, R. Casparis, M. Preiswerk, H. Rudin,  
R. Wagner, P. Zupranski\*

The analyzing power  $A_y$  which is observed in the scattering of neutrons (10 - 30 MeV) from protons can be described by the expression

$$\sigma_0(\theta)A_y(\theta) = \frac{3\sin\theta}{k^2} \sin^2\delta_0, \{ \Delta_{LS}^P + 5\Delta_{LS}^D \cos\theta \}$$

A measurement of the analyzing power at an angle of  $\theta_{CM} = 90^\circ$  gives the possibility to determine the spin-orbit coupling term  $\Delta_{PS}^L$  for p-waves. An atomic beam source produced polarized deuterons ( $\sim 0.5 \mu A$ ) and the  $T(\vec{d}, \vec{n})^4He$ -reaction was used at a deuteron energy of 140 keV as a source of highly polarized 14.2-MeV-neutrons.

The neutron polarization ( $P_n = 0.53 \pm 0.02$ ) was measured with a high pressure scintillation chamber. The proton analyzing power was determined using an associated particle time of flight system.

The measurements of the asymmetry of the neutrons scattered at an angle  $\theta_{CM} = 90^\circ$  were made with cylindrical scatterers of different diameters. The measurements using the bigger scatterers ( $\emptyset = 3.81$  cm) gave an average value of the analyzing power of  $A = (2.12 \pm 0.22)\%$  which is in good agreement with earlier data [1] in this energy region. On the other hand the measurements with the smaller scatterer ( $\emptyset = 2$  cm) gave an average value of the analyzing power of  $A = (0.22 \pm 0.36)\%$ . We suppose that the measurements with the bigger scatterers are strongly influenced and masqued

by multiple scattering effects from the carbon of the scattering scintillators.

#### References

- {1} G. S. Mutchler, J. E. Simmons, Phys. Rev. C4 (1971) 67,  
R. Garret et al., University of Auckland, New Zealand  
(Private Communication)

\* On leave from Instytut Badań Jądrowych, Warschau

#### 2. Analyzing Power of $\vec{n}$ -d-Scattering at 14.2 MeV

M. Preiswerk, R. Casparis, B. Leemann, H. Rudin  
R. Wagner, P. Zupranski\*

We have measured the angular distribution of the analyzing power of deuterium for polarized 14.2-MeV-neutrons. There is a considerable lack of data in this energy range. Accurate data would be very helpful for a theoretical approach to the three nucleon system. Polarized deuterons ( $\sim 0.5 \mu\text{A}$ ) were produced with an atomic beam source and the  $T(\vec{d}, \vec{n})^4\text{He}$ -reaction was used as a source of highly polarized neutrons. The results of our asymmetry measurements are in good agreement with the experimental  $\vec{p}$ -d-data at 14.5 MeV of Faivre et al. {1} and also with the theoretical  $\vec{n}$ -d-predictions of Pieper {2}. (Fig. 1/2)

#### References

- {1} J. C. Faivre et al., Nucl. Phys. A127 (1969) 169  
{2} S. C. Pieper, Nucl. Phys. A193 (1972) 529  
{3} P. Doleschall, Nucl. Phys. A201 (1972) 264

\* On leave from Instytut Badań Jądrowych, Warschau



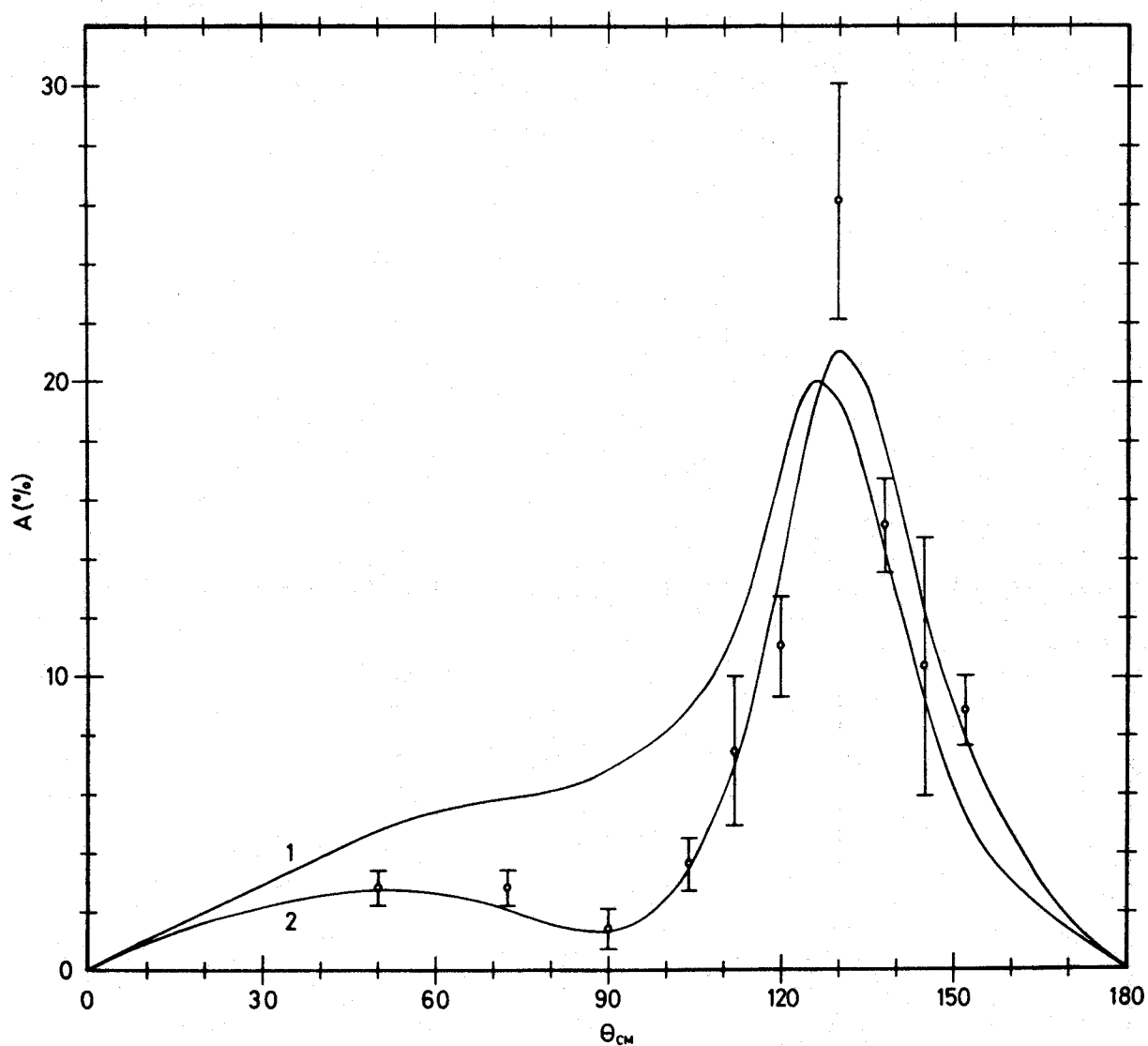


Fig. 1: Comparison of our measurements of the analyzing power of deuterium for polarized 14.2-MeV-neutrons with the theoretical curves of Doleschall {1} and Pieper {2}. The perturbation method of Pieper gives better agreement with the measurements than the calculations of Doleschall {3} which use the solution of the Faddeev-equations. The experimental points are shown with their statistical errors.

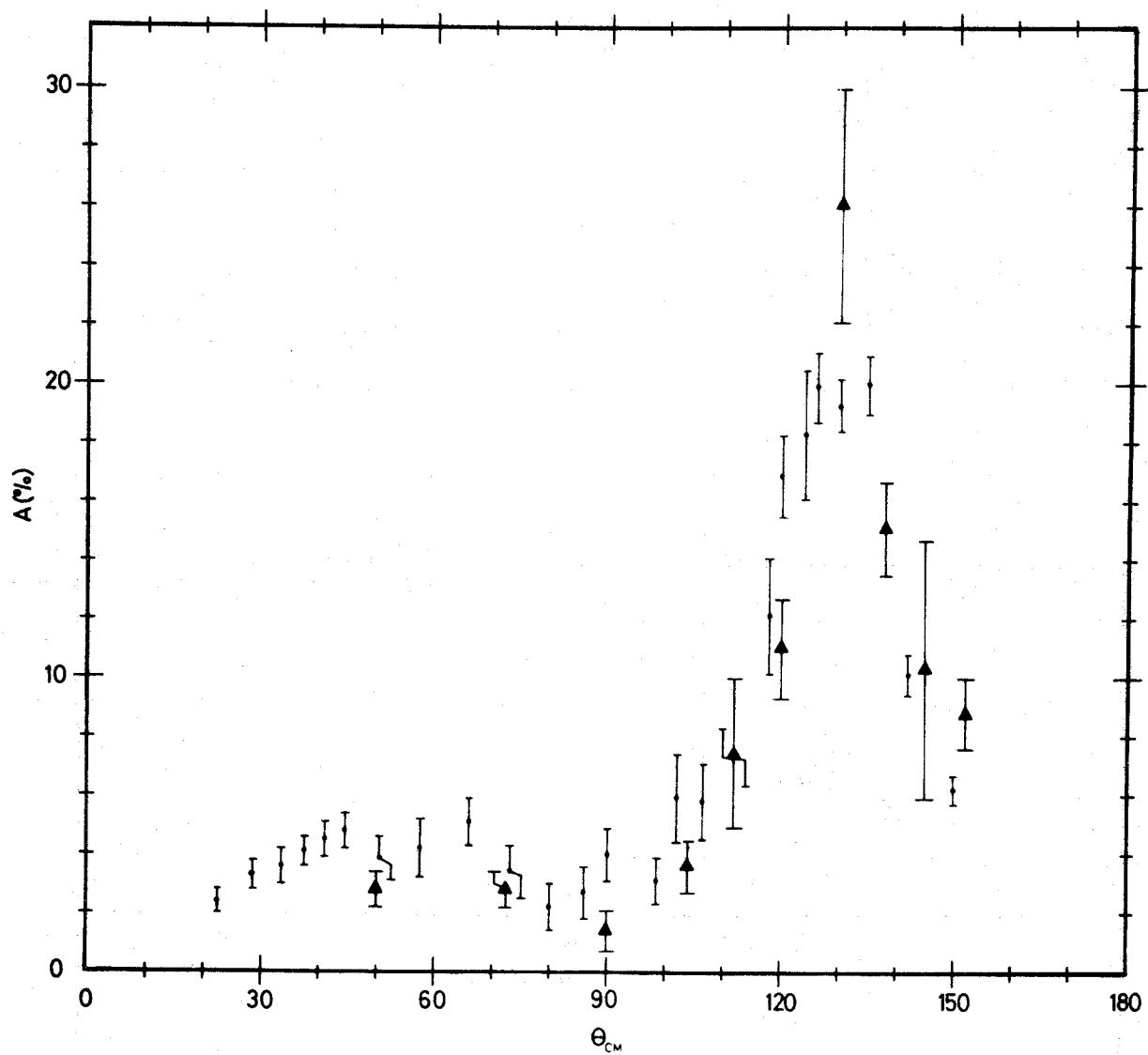


Fig. 2: Comparison of our  $\vec{n}$ -d-results (triangles) with the experimental  $\vec{p}$ -d-data (points) at 14.5 MeV of Faivre.

### 3. Scattering of 14-MeV Polarized Neutrons by $^{12}\text{C}$

R. Casparis, M. Preiswerk, H. Rudin, R. Wagner,  
P. Zupranski\*

At  $E_n = 14.2$  MeV measurements of the angular distribution of the asymmetry  $A(\theta)$  for the  $^{12}\text{C}(n,n')^{12}\text{C}^*$ -inelastic-scattering ( $Q = -4.43$  MeV) and the neutron polarization  $P(\theta)$  for elastic scattering are in progress. The polarized neutrons are produced with the  $T(\vec{d}, \vec{n})^4\text{He}$ -reaction using polarized deuterons. A time of flight technique allows separation of elastically and inelastically scattered neutrons. Up to  $90^\circ$  (Lab) a graphite cylinder serves as scatterer, above  $90^\circ$  carbon recoils in a plastic scintillator give an additional information. The experimental results for the neutron polarization in the elastic scattering are in good agreement with data of Mack et al. {1} and also with comparable  $^{12}\text{C}(p,p)^{12}\text{C}$ -data {2}. The measured asymmetry  $A(\theta)$  of the inelastic scattering shows a similarity with  $^{12}\text{C}(p,p')^{12}\text{C}^*$ -scattering results {2} up to  $90^\circ$  but deviates from this behaviour for larger angles.

#### References

- {1} Mack et al., Proc. 3rd Symp. Polarization Phenomena, Madison (1970), p. 615
- {2} Darriulat et al., Proc. 2nd Symp. Polarization Phenomena, Basel (1966) p. 342

\* On leave from Instytut Badań Jądrowych, Warschau

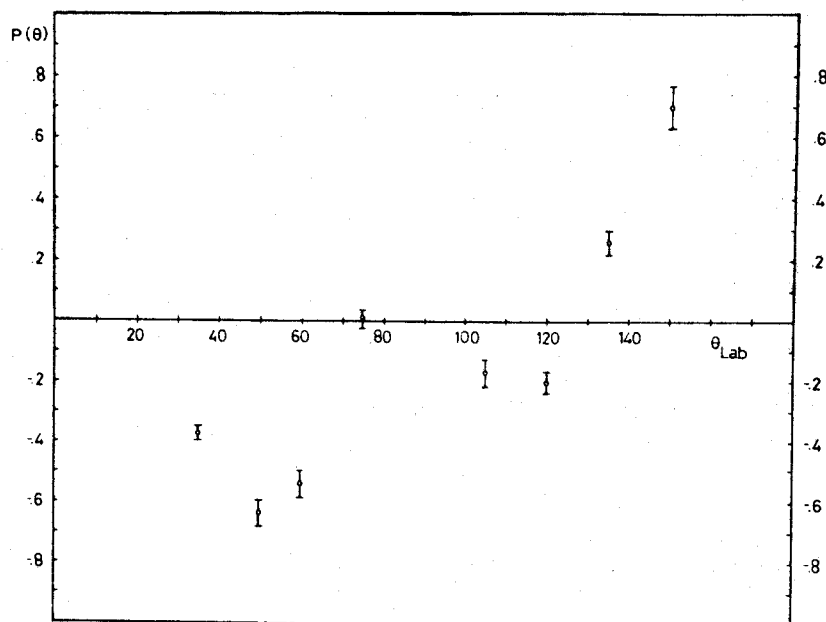


Fig. 1: Polarization  $P(\theta)$  of the  $^{12}\text{C}(n,n)^{12}\text{C}$ -scattering,  
 $E_n = 14.2$  MeV

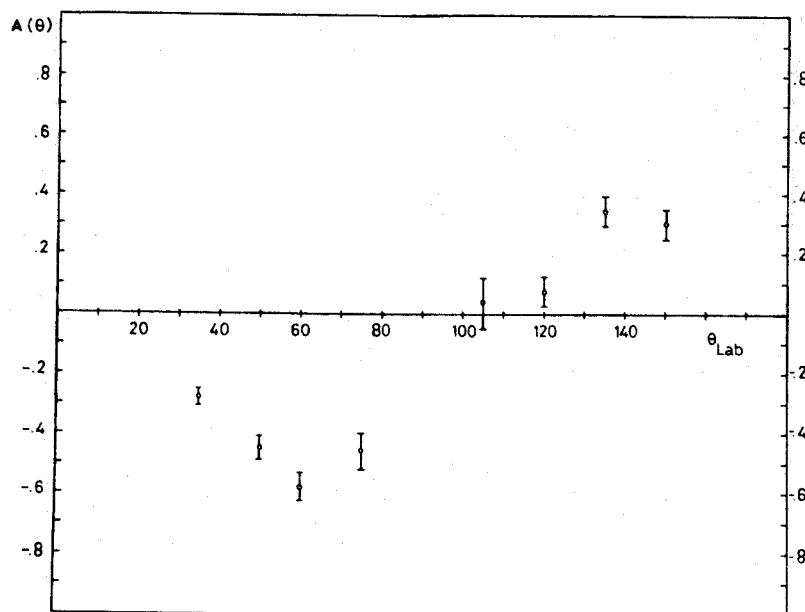


Fig. 2: Asymmetry  $A(\theta)$  of the  $^{12}\text{C}(n,n')^{12}\text{C}^*$ -scattering  
 $(Q = -4.43$  MeV) at  $E_n = 14.2$  MeV

4. Fragment Anisotropy at the  $^{238}\text{U}(n,2nf)$ -Threshold

R. Abegg and R. Wagner

Angular distributions of fragments from neutron induced fission of  $^{238}\text{U}$  have been measured in the energy region  $13.5 \leq E_n (\text{MeV}) \leq 17.5$ . The experimental results show a strong rise in the anisotropy  $A = W(0^\circ)/W(90^\circ) - 1$  (fig. 1) at the thrid-chance fission threshold.

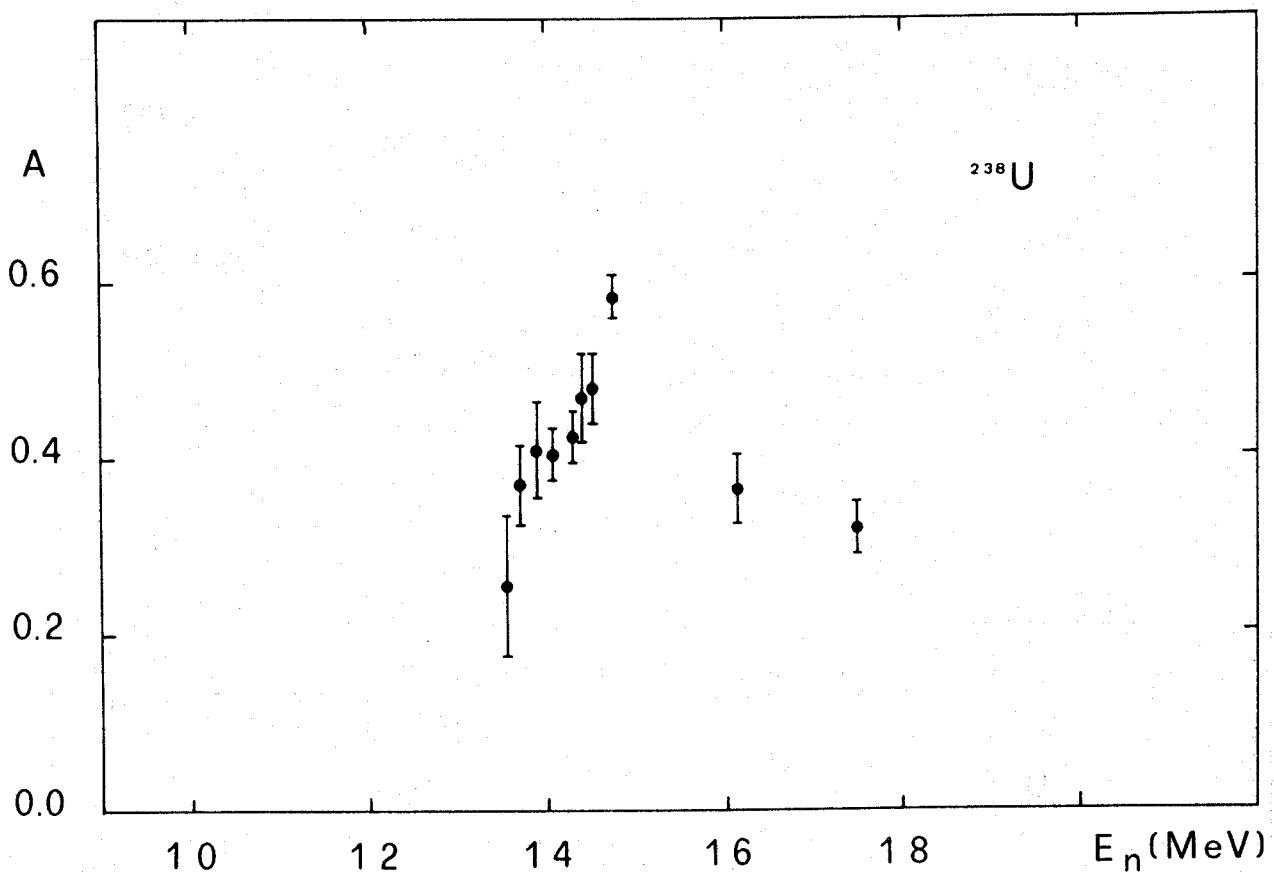


Fig. 1: Anisotropy  $A$  versus neutron energy  $E_n$  (MeV)

The behaviour of the anisotropy in this energy region has been analyzed in the framework of the statistical model. The excitation function of the quantity  $K_0^2$ , which determines the angular momentum distribution along the symmetry axis of the compound nucleus  $^{237}\text{U}$ , as well as the energy dependence of the nuclear temperature  $T$  have been calculated (fig. 2).

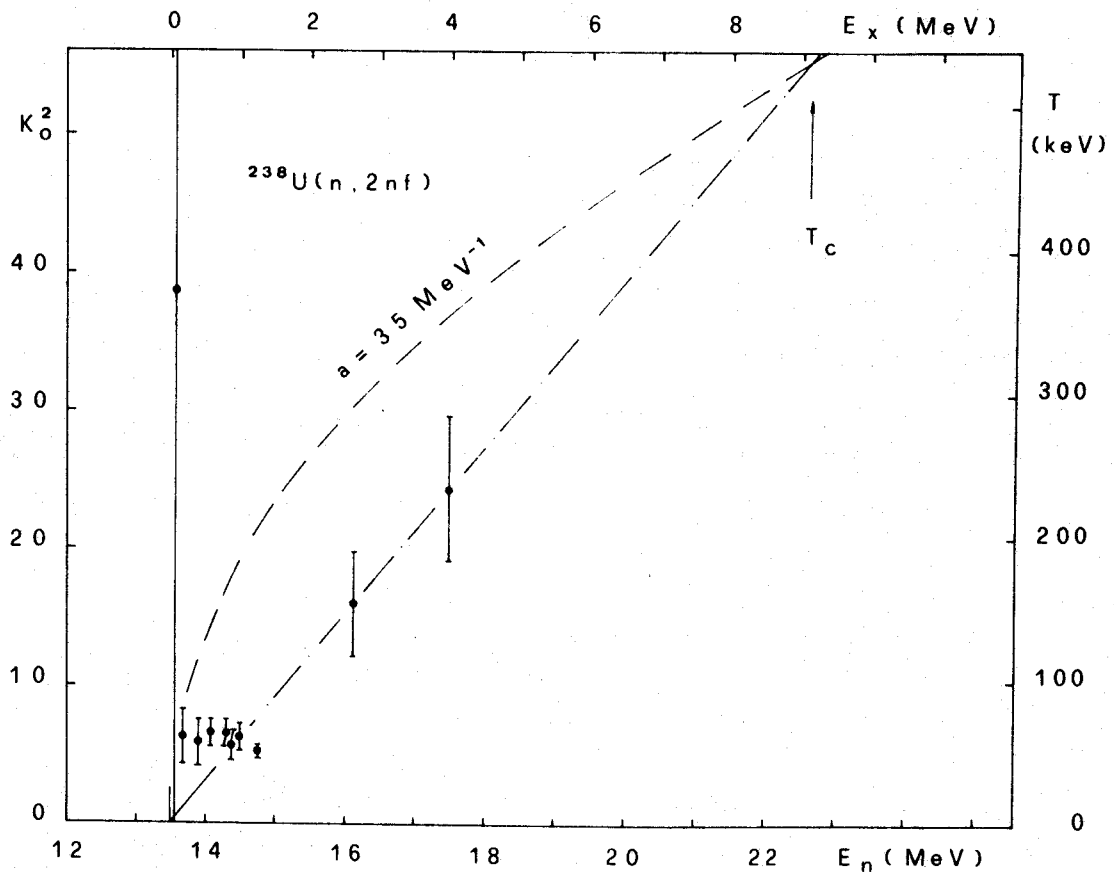


Fig. 2: Energy dependence of  $K_0^2$  and of the nuclear temperature  $T$ .  $E_x$  represents the excitation energy above the (n,2nf)-threshold. ---  $E_x = aT^2 - T$  with a level density parameter of  $35 \text{ MeV}^{-1}$ . -.- linear dependence of  $T$  on  $E_x$  as predicted by the BCS-Model.  $T_c$  : transition energy of the  $^{237}\text{U}$ -nucleus corresponding to an "energy gap" of  $\Delta = 1.8 \pm 0.3 \text{ MeV}$ .

5. (d,p) - stripping reactions on nickel isotopes

P. Staub, H. Schär and E. Baumgartner

The differential cross sections for (d,p)-reactions on  $^{58}\text{Ni}$ ,  $^{60}\text{Ni}$ ,  $^{62}\text{Ni}$  and  $^{64}\text{Ni}$  were measured at 2.8 MeV.

The proton energy spectra were fitted by a special "Gauss-fit" program. Parameters of the optical model derived from elastic scattering data were used for calculating the (d,p) cross sections by means of DWBA (DWUCK). Spectroscopic factors were obtained for approx. 20 excited states in the nickel isotopes.

6. Proton-Proton Scattering in the Energy Range  
500-2000 keV

H. Wassmer, H. Mühry

Precise differential cross sections for proton-proton scattering have been measured at the energies 1.881 MeV, 0.992 MeV and 0.499 MeV simultaneously at angles  $24^\circ$ ,  $50^\circ$  and  $90^\circ$  in the centre-of-mass system. The total uncertainties vary from about 0.1 % at 1.881 MeV and 0.992 MeV to 0.8 % at 0.499 MeV and  $90^\circ$ . A satisfactory agreement between a phase shift analysis and the data can only be obtained by introducing a 'strength factor'  $\Lambda$  for the vacuum-polarization contribution.

A detailed paper has been published in *Helv. Phys. Acta* 46 (1973), 626

1.      Deuteron break-up and proton scattering on  $^{58}\text{Ni}$

A. Buta\*, J. Lang, S. Micek\*\*, R. Müller,  
J. Unternährer and P. Viatte

The break-up of deuterons on  $^{58}\text{Ni}$  has been measured. Contrary to gold the energy-angle correlation of this process shows pronounced structure due to excitation of levels in the intermediate configuration  $^{59}\text{Cu}$ . The proton spectra are confronted with the excitation curves of the proton scattering on the same target.

A detailed paper has been submitted for publication in Physics Letters B.

\*      On leave from Institute for Atomic Physics, Bucarest, Romania

\*\*     On leave from Jagellonian University, Cracow, Poland



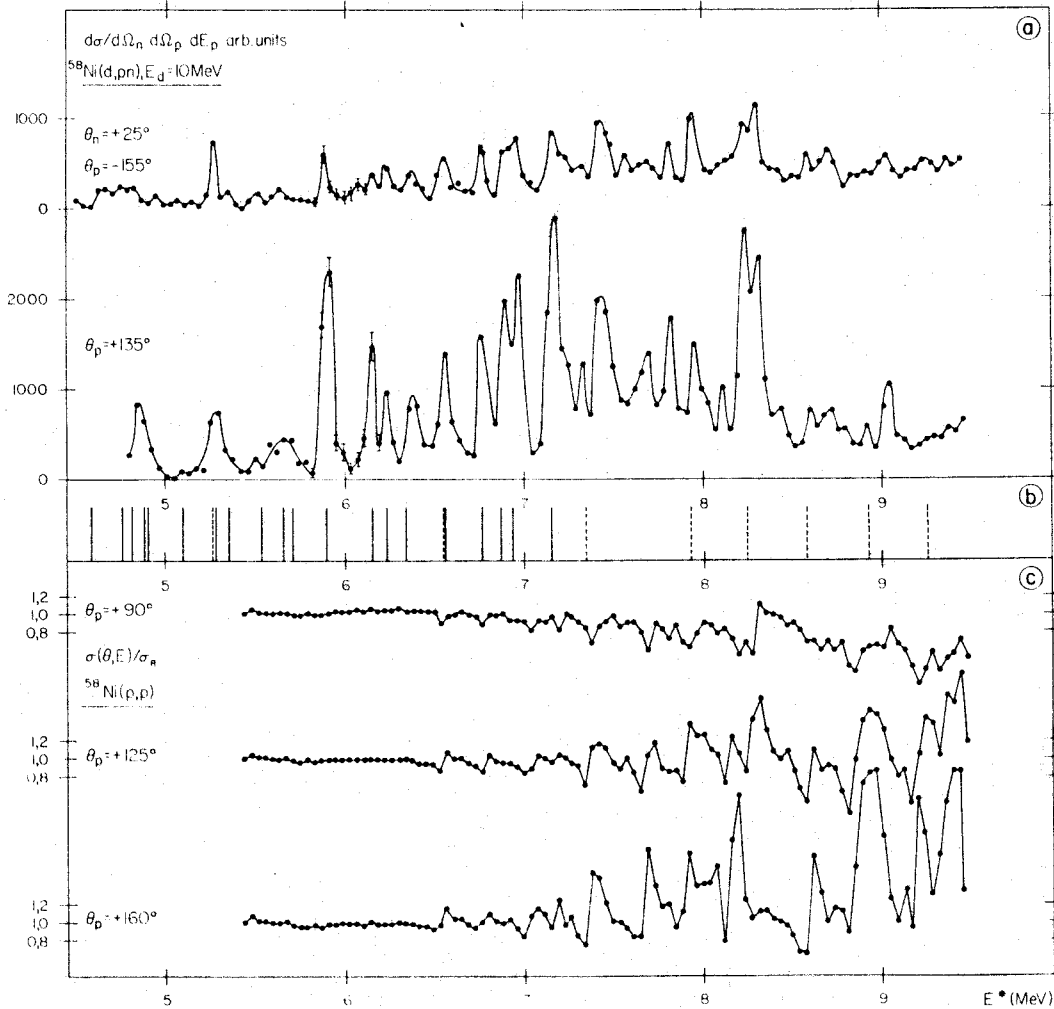


**Fig. 1:** a. Proton spectra  $d\sigma/d\Omega_n d\Omega_p dE_p$  for the reaction  $^{58}\text{Ni}(d, pn)^{58}\text{Ni}$  with  $E_d = 10$  MeV, at the neutron emission angle  $\theta_n = 25^\circ$  and for the proton angles  $\theta_p = +135^\circ$  (proton counter placed on the same side of the beam as the neutron counter) and  $\theta_p = -155^\circ$  (opposite side). As in all other figures in the x-axis the excitation energy of  $^{59}\text{Cu}$  is plotted.

b. Levels in  $^{59}\text{Cu}$   
 ——— ref.5, - - -  $E^* < 7$  MeV: ref.7,  $E^* > 7$  MeV: ref. 6.

c. Excitation curves (cross section divided by Rutherford cross section) for proton elastic scattering on  $^{58}\text{Ni}$  at the angles  $90^\circ$ ,  $125^\circ$ ,  $160^\circ$ , for proton energies from 2 to 6 MeV.

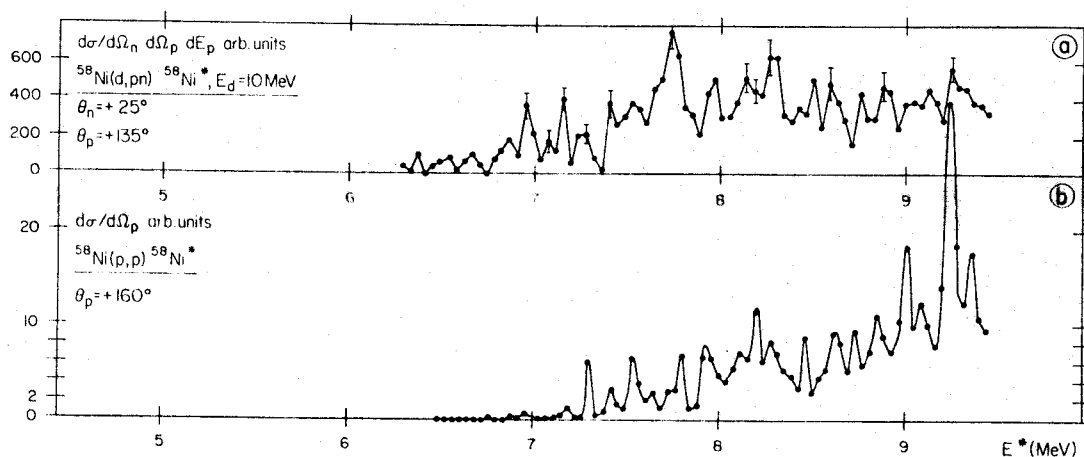


Fig. 2: a. Differential cross section  $d\sigma/d\Omega_n d\Omega_p dE_p$  for break-up on  $^{58}\text{Ni}$  leading to the first excited state of the target nucleus with  $E_d = 10$  MeV, neutron angle  $\theta_n = 25^\circ$ , and proton angle  $\theta_p = +135^\circ$ .  
 b. Excitation function of the inelastic scattering  $^{58}\text{Ni}(p, p')^{58}\text{Ni}^*$  at  $160^\circ$  with excitation of the first  $2^+$  level.

## 2. Calibration of a Neutron Detector

J. Unternährer, J. Lang, R. Müller, P. Viatte

The sensitivity of a neutron detector, consisting of a NE 213 liquid scintillator and a XP 1040 photo multiplier was measured and calculated for neutrons in the energy range 0.4 MeV to 5 MeV. Pulse height was discriminated at 60 keV equivalent electron energy (Am-bias). To determine source strength the  $^2\text{H}(d, n)^3\text{He}$  and  $^3\text{H}(p, n)^3\text{He}$  reactions were counted by the method of associated particles. For the calculations a Monte-Carlo-program was used. Five different processes of energy loss of neutrons within the scintillator were taken into account. Most important are elastic collisions with hydrogen and carbon atoms.

3. Investigation of the  ${}^6\text{Li}(\text{d},\alpha){}^4\text{He}$  Reaction by Polarized Deuterons

R. Risler, W. Grüebler, A. A. Debenham, V. König,  
D. Boerma and P. A. Schmelzbach

The nucleus  ${}^8\text{Be}$  is of great theoretical interest since it is considered to have a simple alpha-particle like structure. This clustering is expected for at least the states with low excitation energy but also states at higher energy are likely to have a quartet configuration. Below an excitation energy of 16 MeV the level structure seems to be well understood. Above this energy the level structure becomes more complex as other configuration like  $\text{p} + {}^7\text{Li}$ ,  $\text{n} + {}^6\text{Li}$  are also important.

In the last few years much experimental evidence for highly excited states in  ${}^8\text{Be}$  has been found. Phase shift analysis of  $\alpha$ - $\alpha$  scattering seems to give the best information on levels with alpha-particle configuration [1]. However levels having other configurations are mostly detected by the absorption part of the phase shifts and are shown only very weak if the transition to this configuration is small. Also high spin levels, particularly the broad ones, would be difficult to observe experimentally by  $\alpha$ - $\alpha$  scattering. In these cases a resonance will escape observation since the change in the corresponding phase shift would be very weak.

The  ${}^7\text{Li}(\text{p},\alpha){}^4\text{He}$  and the  ${}^6\text{Li}(\text{d},\alpha){}^4\text{He}$  reactions have been the favorites in order to study the even spin and parity levels, because their spin structure is relatively simple, due to the two identical spinless particles in the exit channel. Most of these experimental results consist of differential cross section data and measurements with vector polarized proton and deuteron beams. Over a very limited deuteron energy range (0.40 to 0.96 MeV)

corresponding to an excitation energy in  ${}^8\text{Be}$  from 22.6 to 23.0 MeV, tensor analysing power measurements of the  ${}^6\text{Li}(\text{d},\alpha){}^4\text{He}$  reaction were reported.

In spite of the large amount of experimental data ambiguous assignments have come from the different analyses. All R-matrix and S-matrix analyses of the above mentioned reactions require at least three levels in  ${}^8\text{Be}$  between 22 and 26 MeV excitation energy in order to explain the experimental data. Several level sequences with  $0^+$ ,  $2^+$  and  $4^+$  states are proposed {2} all fitting the differential cross section equally well. On the other hand the polarization data are too scarce in order to differentiate between these different assignments.

The  $\alpha$ - $\alpha$  phase shift analysis shows clear evidence for a  $2^+$  doublet near 17 MeV and three states with  $4^+$ ,  $2^+$  and  $0^+$  around 20 MeV excitation energy, however the higher states show up less convincing. At excitation energies higher than 26 MeV no indications for further resonances exist.

This unsatisfactory situation suggests that more experimental information is needed for a final assignment of the level structure at energies higher than 20 MeV. The particles in the entrance channel of the  ${}^6\text{Li}(\text{d},\alpha){}^4\text{He}$  reaction have a binding energy of 22.28 MeV above the ground state of  ${}^8\text{Be}$ . The necessary information for an improved R-matrix analyses could be provided by measurements of vector and tensor analysing powers over an extended energy range. Recently it has been shown that these quantities can reveal essential information on the level structure in the corresponding compound nucleus {3}.

In the present work data on the cross section, the vector analysing power  $iT_{11}$  and the three tensor analysing powers  $T_{20}$ ,  $T_{21}$  and  $T_{22}$  in the energy range between 1.5 and 11.5 MeV are reported. The results are shown in figs. 1 to 5.

### References

- {1} A. D. Bacher, F. G. Resmini, H. E. Conzett, R. de Swiniarski,  
H. Meiner and J. Ernst, Phys. Rev. Lett. 29 (1972) 1331
- {2} Tsan Ung Chan, J. P. Longequeue and H. Beaumevieille,  
Nucl. Phys. A 124 (1969) 449
- {3} F. Seiler, Nucl. Phys. A 187 (1972) 379

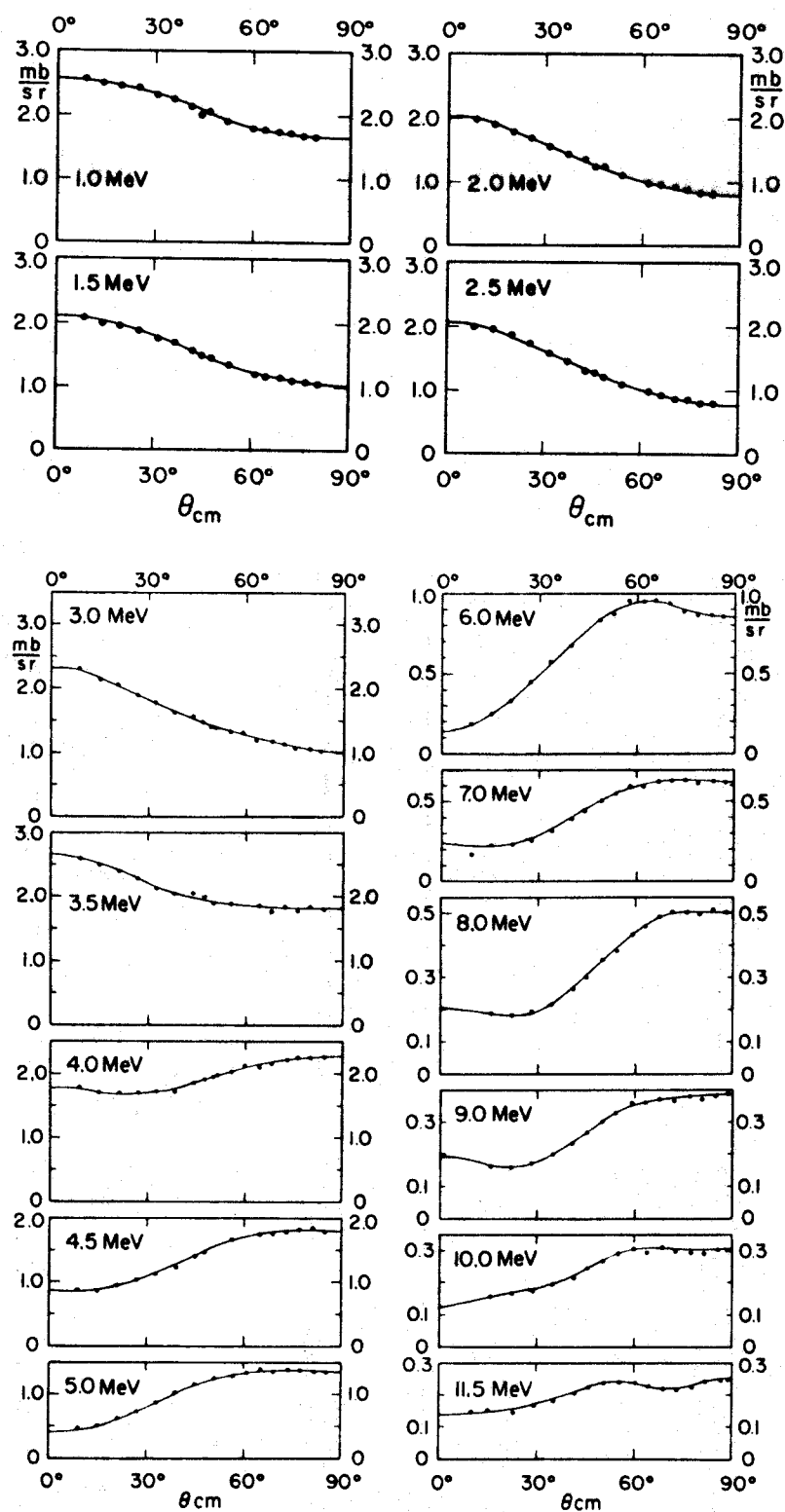


Fig. 1: Angular distributions of the cross section for the  ${}^6\text{Li}(d,\alpha){}^4\text{He}$  reaction

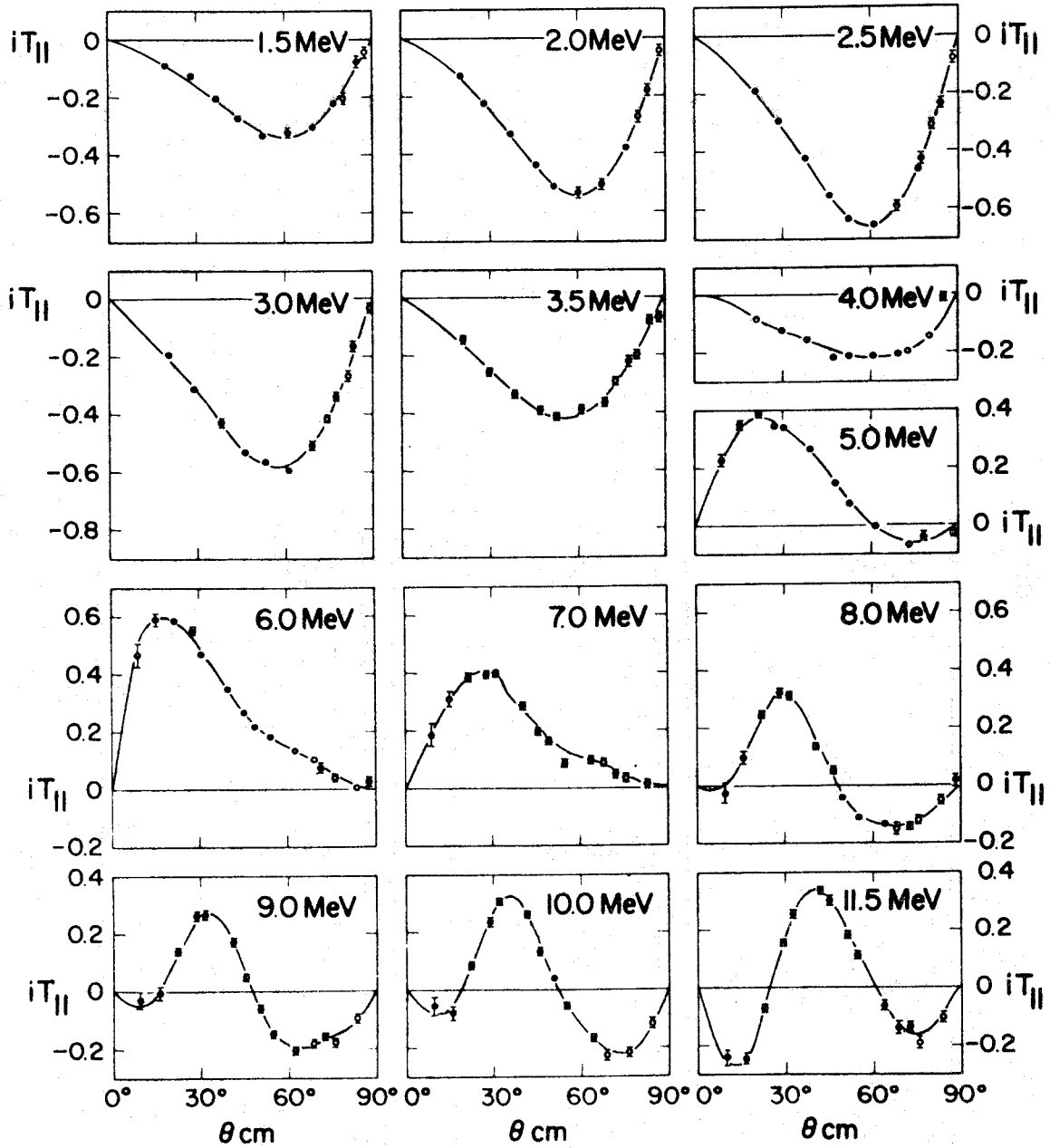


Fig. 2: The vector analysing power  $iT_{11}$

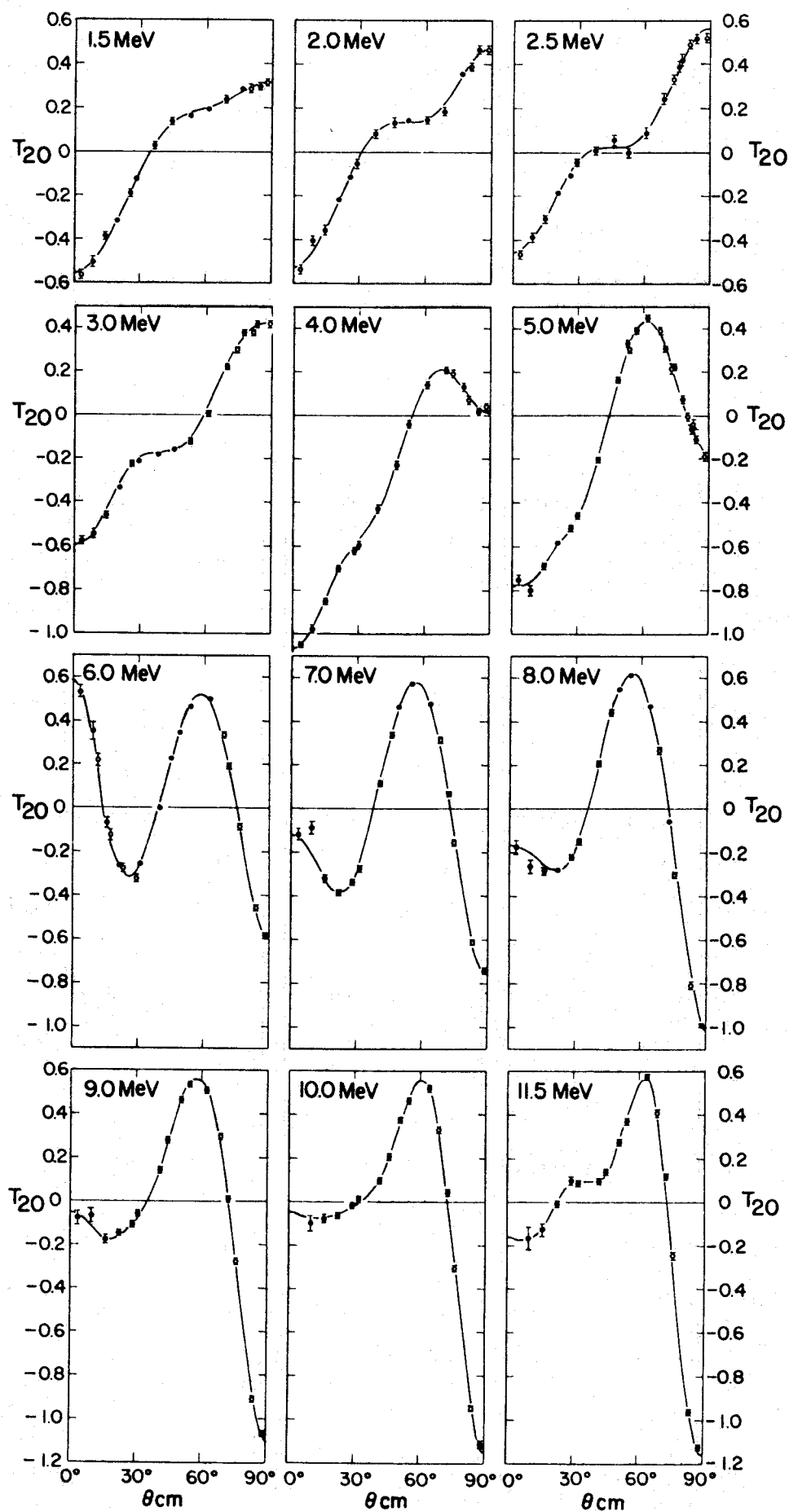


Fig. 3: The tensor analysing power  $T_{20}$



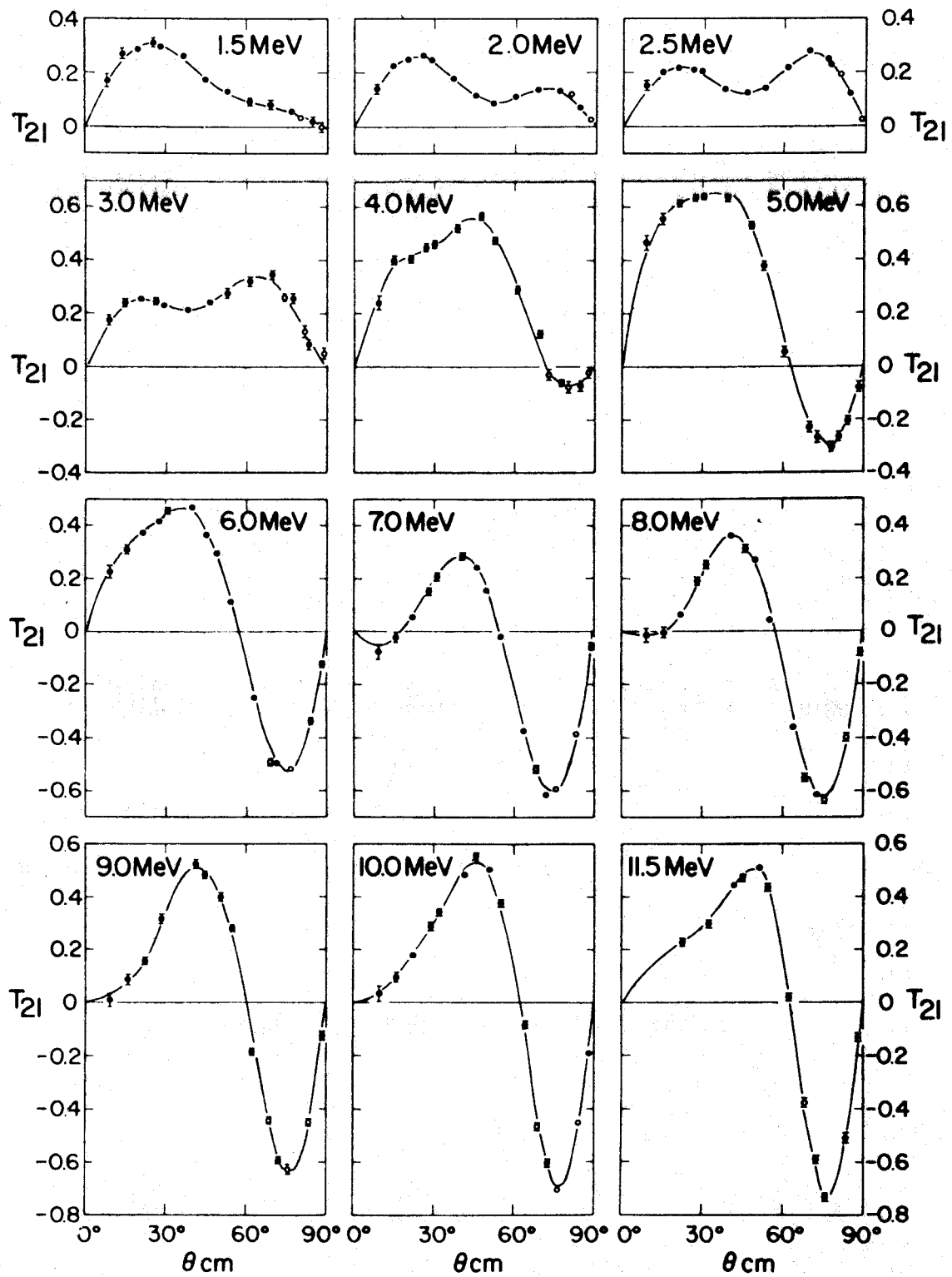


Fig. 4: The tensor analysing power  $T_{21}$

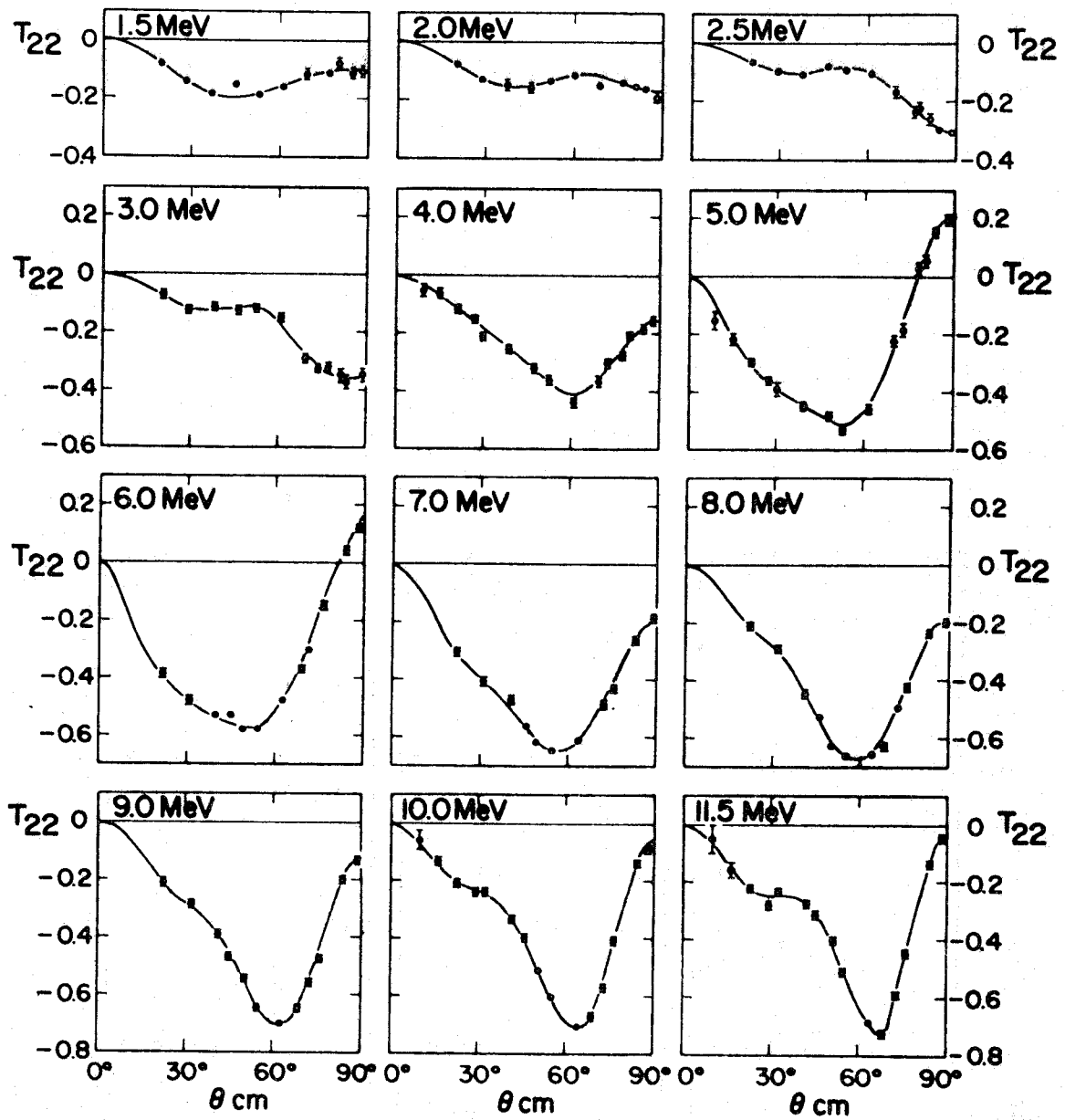


Fig. 5: The tensor analysing power  $T_{22}$

VII. Institut de Physique Nucléaire, Université de  
Lausanne

---

(Dir.: Prof. Dr. M. Gaillard)

1. (n,p), (n,d), (n,t) and (n, $\alpha$ ) Reactions at 14 MeV

Ch. Sellem and J. P. Perroud

The experimental results have been analyzed by means of two identification methods. The first, simple method yields the differential cross section in mb/sr.

a)  $^{10}\text{B} (n, \alpha_0 + \alpha_1) ^7\text{Li}$  and  $^{10}\text{B} (n, \alpha_2) ^7\text{Li}^*$  reactions:

$\theta_{\text{Lab}}$ (deg)	20	40	60	80	100	120	137
$(n, \alpha_0 + \alpha_1)$ ( $\pm 0.09$ )	0.83 ( $\pm 0.09$ )	0.62 ( $\pm 0.06$ )	1.1 ( $\pm 0.06$ )	1.0 ( $\pm 0.09$ )	0.8 ( $\pm 0.08$ )	1.2 ( $\pm 0.09$ )	1.8 ( $\pm 0.16$ )
$(n, \alpha_2)$ ( $\pm 0.2$ )	3.8 ( $\pm 0.2$ )	1.8 ( $\pm 0.1$ )	1.5 ( $\pm 0.1$ )	1.2 ( $\pm 0.08$ )	1.3 ( $\pm 0.07$ )	1.8 ( $\pm 0.1$ )	3.5 ( $\pm 0.2$ )

b)  $^{10}\text{B} (n, t_0) ^8\text{Be}$  reaction:

$(n, t_0)$ ( $\pm 0.1$ )	0.56 ( $\pm 0.1$ )	0.2 ( $\pm 0.04$ )	0.3 ( $\pm 0.06$ )	0.44 ( $\pm 0.06$ )			
-----------------------------	-----------------------	-----------------------	-----------------------	------------------------	--	--	--

c)  $^{10}\text{B} (n, d_0) ^9\text{Be}$  and  $^{10}\text{B} (n, d_1) ^9\text{Be}^*$  reactions:

$\theta_{\text{Lab}}$ (deg)	20	20	60	80	100	120	137
$(n, d_0)$	5.67 ( $\pm 0.3$ )	1.9 ( $\pm 0.2$ )	1.9 ( $\pm 0.1$ )				
$(n, d_1)$	3.9 ( $\pm 0.25$ )	1.1 ( $\pm 0.1$ )					

d)  $^{10}\text{B} (n, p_0) ^{10}\text{Be}$  and  $^{10}\text{B} (n, p_1) ^{10}\text{Be}^*$  reactions:

$(n, p_0)$	0.16 ( $\pm 0.02$ )	0.14 ( $\pm 0.04$ )	0.13 ( $\pm 0.05$ )	0.13 ( $\pm 0.05$ )			
$(n, p_1)$	1.1 ( $\pm 0.1$ )	1.0 ( $\pm 0.08$ )	0.75 ( $\pm 0.09$ )	0.65 ( $\pm 0.09$ )			

It is found that

- For the  $^{10}\text{B} (n, \alpha_0 + \alpha_1) ^7\text{Li}$  and  $^{10}\text{B} (n, \alpha_2)$  reactions our measured cross sections are  $\sim 30\%$  higher than the results reported by Antolkovic et al. [1], whose measurements were performed only up to  $90^\circ$  (CM).
- For the (n,p) and (n,d) reactions our results are  $30\%$  lower than those reported by Valkovic et al. [2]. Their measurements were performed over the angular range  $0^\circ$ - $130^\circ$  (CM).
- For the (n,t) reactions our results are  $20\%$  lower than those reported by Valkovic [3] which were measured up to  $130^\circ$  (CM).

A more sophisticated identification method will yield the remaining cross sections in the  $0-137^\circ$  (Lab) range shortly.

The full results and a discussion of the discrepancy with respect to the authors quoted will be reported. {4} and {5}.

The apparatus used and the identification methods will be described in a subsequent paper {6}.

#### References

- {1} B. Antolkovic, J. Huldomalj, B. Janko, G. Paic and M. Turk, Nucl. Phys. A 139 (1969) 10-16
- {2} V. Valkovic, P. Thomas, J. Slaus and M. Cerineo, Glasnik Matematicko-Fisicki i Astronomski. Tom 19, No. 3-4
- {3} V. Valkovic, Nucl. Phys. 54 (1964) 465-471
- {4} Ch. Sellem, Thesis (to be submitted to EPFL)
- {5} to be submitted to Helv. Phys. Acta
- {6} to be submitted to Nucl. Instr. & Methods